GLOBAL PRECIPITATION MEASUREMENT (GPM) MISSION

Algorithm Theoretical Basis Document

Version **B2**

April 30th, 2013

Passive Microwave Algorithm Team Facility

TABLE OF CONTENTS

GLOSSARY OF ACRONYMS

A

Advanced Microwave Scanning Radiometer for the Earth observing system (AMSR-E)

Advanced Microwave Sounding Unit (AMSU)

ATBD (Algorithm Theoretical Basis Document)

D

Dual Frequency Radar (DFR)

E

European Centre for Medium-Range Weather Forecasts (ECMWF)

G

GANAL (JMA Global ANALysis)

Global Data Assimilation System (GDAS)

GMI (GPM Microwave Imager)

GPM (Global Precipitation Measurement)

GPM Microwave Imager (GMI)

Goddard Profiling Algorithm (GPROF)

Ground Validation (GV)

Goddard Multi-scale Modeling Framework (MMF)

I

Interactive Multi-sensor Snow and Ice Mapping System (IMS)

L

Land Surface Model (LSM)

M

Moderate Resolution Imaging Spectroradiometer (MODIS)

N

National Centers for Environmental Prediction (NCEP)

National Snow and Ice Data Center (NSIDC)

NOAA National Mosaic and Multi-Sensor QPE (NMQ)

Numerical weather prediction (NWP)

P

Precipitation Processing System (PPS)

Passive microwave retrieval (PWR)

Precipitation radar (PR)

S

Special Sensor Microwave/Imager (SSM/I)

Special Sensor Microwave Imager / Sounder (SSMIS)

T

Brightness temperature (T_b)

Total Column Water Vapor (TCWV)

Tropical Rainfall Measuring Mission (TRMM)

Tropical Rainfall Measuring Mission - Microwave Imager (TMI)

Skin Temperature (TSKIN)

1.0 INTRODUCTION

1.1 Objectives

The Global Precipitation Measurement (GPM) Mission is an international space network of satellites designed to provide the next generation precipitation observations every two to four hours anywhere around the world. GPM consists of both a defined satellite mission and a collaborative effort involving the global community. The GPM concept centers on the deployment of a "Core" observatory carrying advanced active and passive microwave sensors in a non-Sun-synchronous orbit to serve as a physics observatory to gain insights into precipitation systems and as a calibration reference to unify and refine precipitation estimates from a constellation of research and operational satellites. As a science mission with integrated applications goals, GPM will advance understanding of the Earth's water and energy cycle and extend current capabilities in using accurate and timely information of precipitation to directly benefit the society. The current Algorithm Theoretical Basis Document (ATBD) deals with the Passive Microwave Algorithms associated with the GPM mission. The passive microwave algorithm is designed to take advantage of the Core observatory to define *a-priori* databases of observed precipitation profiles and their associated brightness temperature signals. These databases are then used in conjunction with Bayesian inversion techniques to build consistent retrieval algorithms for the Core satellite's GMI instrument and each of GPM's constellation satellites. The specific implementation is described below.

1.2 Purpose

This ATBD describes the Global Precipitation Measurement (GPM) passive microwave rainfall algorithm, which is a parametric algorithm used to serve all GPM radiometers. The output parameters of the algorithm are enumerated in Table 1. The algorithm is based upon the concept that the GPM core satellite, with its Dual Frequency Radar (DPR) and GPM Microwave Imager (GMI), will be used to build a consistent *a-priori* database of cloud and precipitation profiles to help constrain possible solutions from the GMI radiometer beyond the swath of the radar as well as the constellation radiometers.

In particular, this document identifies the physical theory upon which the algorithm is based and the specific sources of input data and output from the retrieval algorithm. The document includes implementation details, as well as the assumptions and limitations of the adopted approach. Because the algorithm is being developed by a team of scientists, this document additionally serves to keep each developer abreast of all the algorithm details and formats needed to interact with the code. The version number and date of the ATBD will, therefore, always correspond to the version number and date of the algorithm—even if changes are trivial.

Table 1. Key output parameters from the Level 2 Rainfall Product.

Pixel Information		
Parameter	**Units**	**Comments**
Latitude, longitude	Deg.	Pixel earth coordinate position
Surface Type	None	land surface emissivity class/ocean/coast/sea ice
Retrieval Type	None	Identifies if pixel retrieved with S0, S1, or S2
Pixel Status	None	Identifies pixels eliminated by QC procedures
Quality Flag	None	Pixels w/o good T_b matches in database
Skin Temperature Total Column Water Vapor 2 meter temperature	^oK mm ^oK	Pass-through variables from Model
Surface Precipitation	mm/hr	Total Precipitation
Liquid Precip Fraction Convective Precip Fraction	0-1.0 0-1.0	Portion of Surface Precip in Liquid State Portion of Surface Precip that is Convective
Precipitation structure	None	Index for self-similar hydrometeor profiles; 28 layers, separated by hydrometeor species
Precipitation Diagnostics	None	Precip Retrieval diagnostics and uncertainties
Cloud Water Path Rain Water Path Mixed Phase Path Ice Water Path	Kg/m^2	Integrated from retrieved profile

1.3 Scope

This document covers the theoretical basis for the at-launch passive microwave algorithm used by GPM for the retrieval of liquid and solid precipitation from the GMI and constellation radiometers. The GPM radiometer algorithm will be a Bayesian type algorithm. These algorithms search an *a-priori* database of potential rain profiles and retrieve a weighted average of these entries based upon an uncertainty weighted proximity of the observed T_b to the T_b of a set of previously observed rain profiles. By using the same *a-priori* database of rain profiles, with appropriate simulated T_b for each constellation sensor, the Bayesian method is completely parametric and thus well suited for GPM's constellation approach. The *a-priori* information supplied by GPM's core satellite immediately benefits not just the GMI radiometer but all radiometers that form GPM constellations. Because the ultimate objective is to use the DPR and GMI on the GPM core satellite to build this a-priori database, an alternative method to create the database had to be developed for the at-launch algorithm. It is understood that this is not the ideal method but it should be useful to test the truly parametric nature of the algorithm and provide rainfall estimates no worse than our best methods available today.

The mathematics of Bayesian inversions are well understood. The solution provides a mean rain rate as well as its uncertainty. The major sources of systematic errors in these algorithms are the quality of the *a-priori* database; the estimate of the forward model uncertainty; and the ancillary information used to subset the *a-priori* database.

Section 2 provides GPM satellite instrumentation background as well as a list of Constellation radiometers being considered. Details of the constellation radiometers are found in Appendix A.

The process concepts and algorithm descriptions for the geophysical parameters of the rainfall product are presented in Section 3. Section 4 describes the algorithm infrastructure, while Section 5 summarizes the assumptions and limitations and Section 6 discusses the various planned algorithm improvements.

1.4 Changes From Previous Versions

This ATBD represents version B2 (Beta test-2) of the algorithm that was delivered to the Precipitation Processing System on March 31, 2013. As such, it contains details of what was actually implemented in the second "working" version of the algorithm code. The code is parametric to a very large extent, requiring only that channel frequencies, polarizations and uncertainties be entered for each conically scanning radiometer. Cross-track sounder algorithms will be constructed in nearly the same fashion but the addition of large scan angle variations is best handled by separate code that will be described in a new and separate section.

2.0 INSTRUMENTATION

2.1 GPM Core Satelite

The GPM Core Spacecraft will fly two precipitation instruments: the GPM Microwave Imager (GMI) and the Dual-frequency Precipitation Radar (DPR). Together, these instruments will provide a unique capability for measuring precipitation falling as light rain or snow—conditions that have been difficult to detect using previous instruments. Compared to the earlier generation of instruments, the new capabilities of the GMI and DPR are enabled by the addition of high frequency channels (165.6 and 183.3 GHz) on the GMI, and the inclusion of a Ka-band (35.5 GHz) radar on the DPR.

2.1.1 GPM Microwave Imager

The GPM Microwave Imager (GMI) instrument is a multi-channel, conical-scanning, microwave radiometer serving an essential role in the near-global-coverage and frequent-revisit-time requirements of GPM (see Fig. 1). The instrumentation enables the Core spacecraft to serve as both a 'precipitation standard' and as a 'radiometric standard' for the other GPM constellation members. The GMI is characterized by thirteen microwave channels ranging in frequency from

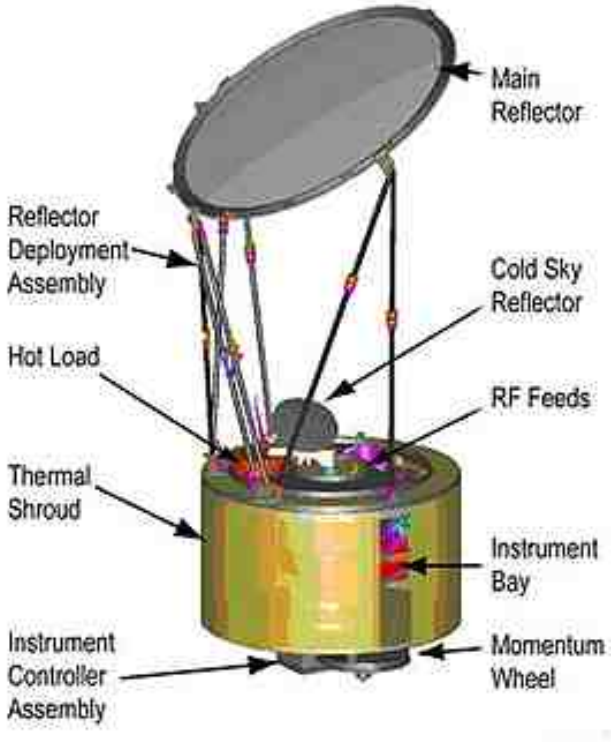

Fig. 1. GMI instrument.

10 GHz to 183 GHz (see Table 2). In addition to carrying channels similar to those on the Tropical Rainfall Measuring Mission (TRMM) Microwave Imager (TMI), the GMI carries four

high frequency, millimeter-wave channels at about 166 GHz and 183 GHz. With a 1.2 m diameter antenna, the GMI will provide significantly improved spatial resolution over TMI. Launch date for the core spacecraft: February, 2014.

Table 2. GMI performance characteristics.

Frequency (GHz)	Polarization	NEDT/ Reqmt (K)	Expected* NEDT	Expected Beam Efficiency (%)	Expected Calibration Uncert.	Resolution (km)
10.65	V/H	0.96	0.96	91.4	1.04	26
18.7	V/H	0.84	0.82	92.0	1.08	15
23.8	V	1.05	0.82	92.5	1.26	12
36.5	V/H	0.65	0.56	96.6	1.20	11
89.0	V/H	0.57	0.40	95.6	1.19	6
165.5	V/H	1.5	0.81	91.9	1.20	6
183.31±3	V	1.5	0.87	91.7	1.20	6
183.31±7	V	1.5	0.81	91.7	1.20	6

2.1.2 Dual-Frequency Precipitation Radar

One of the prime instruments for the GPM Core Observatory is called the Dual-frequency Precipitation Radar (DPR). The DPR consists of a Ku-band precipitation radar (KuPR) and a Ka-band precipitation radar (KaPR). The KuPR (13.6 GHz) is an updated version of the highly successful unit flown on the TRMM mission. The KuPR and the KaPR will be co-aligned on the GPM spacecraft bus such that the 5-km footprint location on the Earth will be the same. Data collected from the KuPR and KaPR units will provide the 3-dimensional observation of rain and will also provide an accurate estimation of rainfall rate to the scientific community. The DPR instrument will be allocated 190 Kbps bandwidth over the 1553B spacecraft data bus. The collection of the DPR data will be transmitted to the ground using the TDRSS multiple access (MA) and single access (SA) services.

The DPR is a spaceborne precipitation radar capable of making accurate rainfall measurements. The DPR is expected to be more sensitive than its TRMM predecessor especially in the measurement of light rainfall and snowfall in the high latitude regions. Rain/snow determination is expected to be accomplished by using the differential attenuation between the Ku-band and the Ka-band frequencies. The variable pulse repetition frequency (VPRF) technique is also expected to increase the number of samples at each IFOV to realize a 0.2 mm/h sensitivity.

The KuPR and KaPR, together with GMI, are the primary instruments on the GPM spacecraft. These Earth-pointing KuPR and KaPR instruments will provide rain sensing over both land and ocean, both day and night. Top-level general design specifications are seen in Table 3 and Fig. 2.

Table 3. DPR performance characteristics.

Item	Swath Width (km)	Range Resolu-tion (m)	Spatial Resolu-tion (km Nadir)	Beam Width (deg)	Trans-mitter (SSA)	Peak Transmit Power (W)	Pulse Repe-tition Freq. (Hz)	Pulse Width	Beam #
KuPR	245	250	5	0.71	128	1000	4100 - 4400	2; 1.667 μs pulses	49
KaPR	120	250/500	5	0.71	128	140	4100 - 4400	2; 1.667 μs pulses in matched beams 2; 3.234 μs pulses in interlaced scans	49 (25 matched beams and 24 interlaced scans)

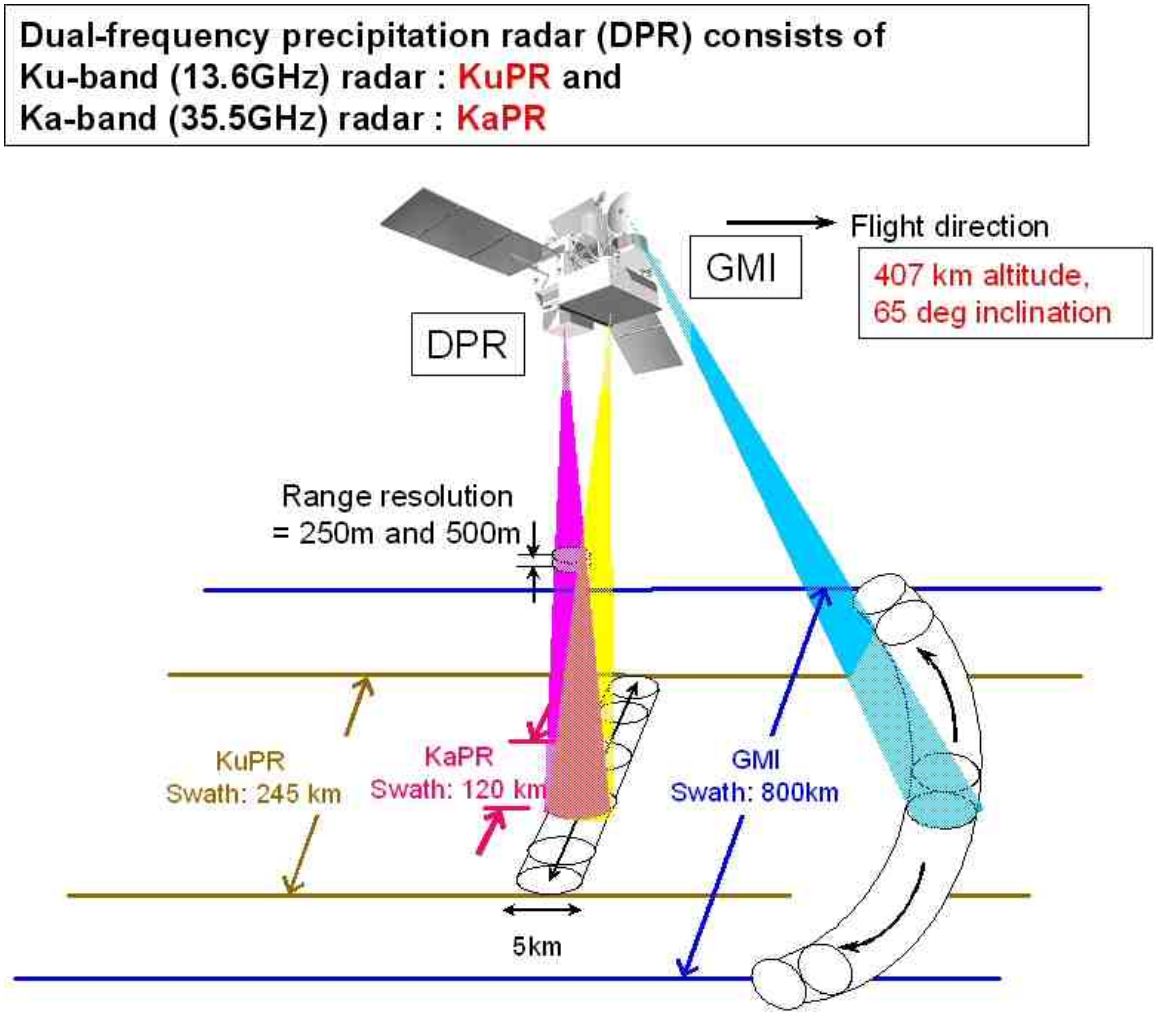

Fig. 2. GPM swath measurements.

2.2 GPM Constellation Satellites

In addition to the core instruments (GMI and DPR) the passive microwave algorithm will make use of several constellation radiometers that have similar channel sets as the GMI radiometer. These constellation radiometers are listed in Table 4 and described in detail in Appendix A.

Table 4. Launch and end dates of constellation radiometers in order of launch

Constellation Radiometers	**Launch Date**	**End Date**
AMSR 2	July 2012	N/A
MADRAS	October 2011	N/A
SAPHIR	October 2011	N/A
SSMIS	F-16: Oct. 18, 2003	Active
	F-17: Nov. 4, 2006	Active
	F-18: Oct. 18, 2009	Active
WindSat	Jan. 6, 2003	Active
AMSR-E	May 4, 2002	Oct. 2011
*AMSU A	NOAA-15 (NOAAK): May 13, 1998	Active
AMSU B	NOAA-16 (NOAAL): Sep. 21, 2000	Active
MHS	NOAA-17 (NOAAM): Jun. 24, 2002	Active
	NOAA-18 (NOAAN): Aug. 30, 2005	Active
	MetOp-A: May 21, 2007	Active
	NOAA-19 (NOAAN'): Jun. 02, 2009	Active
	MetOp: 2012	N/A
ATMS	NPP: 2011	N/A
	JPSS: 2015	N/A
	JPSS: 2018	N/A
TMI	Nov. 27, 1997	Active
SSM/I	F-8: Jun. 20, 1987	Dec. 1991
	F-10: Dec. 1, 1990	Nov. 1997
	F-11: Nov. 28, 1991	May 2000
	F-13: Mar. 24, 1995	Nov. 2009
	F-14: Apr. 4, 1997	Aug. 2008
	F-15: Dec. 12, 1999	** Active

*The AMSU A's and B's have flown together on the 3 NOAA KLM satellites. MHS replaces AMSU-B on NOAA-18 and 19.
**F-15: Beacon corrected data after Aug. 2006.

3.0 THE ALGORITHM

3.1 Theroretical Description

The GPM radiometer algorithm is based upon a Bayesian approach in which the GPM core satellite is used to create an *a-priori* database of observed cloud and precipitation profiles. Once a database of profiles and associated brightness temperatures is established, the retrieval employs a straightforward Bayesian inversion methodology. In this approach, the probability of a particular profile **R**, given $\mathbf{T_b}$ can be written as:

$$\Pr(\mathbf{R} \mid \mathbf{T_b}) = \Pr(\mathbf{R}) \times \Pr(\mathbf{T_b} \mid \mathbf{R}) , \quad (1)$$

where Pr(**R**) is the probability that a certain profile **R** will be observed and Pr($\mathbf{T_b} \mid \mathbf{R}$) is the probability of observing the brightness temperature vector, $\mathbf{T_b}$, given a particular rain profile **R**. The first term on the right hand side of Eqn. (1) is derived from the *a-priori* database of rain profiles established by the radar/radiometer observing systems discussed in section 3.1. The second term on the right hand side of Eqn. (1), is obtained from radiative transfer computations through the cloud model profiles. The formal solution to the above problem is presented in detail in Kummerow *et al*., (1996). In summary, the retrieval procedure can be said to compose a new hydrometeor profile by taking the weighted sum of structures in the cloud structure database that are radiometrically consistent with the observations. The weighting of each model profile in the compositing procedure is an exponential factor containing the mean square difference of the sensor observed brightness temperatures and a corresponding set of brightness temperatures obtained from radiative transfer calculations through the cloudy atmosphere represented by the model profile. In the Bayesian formulation, the retrieval solution is given by:

$$\hat{E}(R) = \sum_j R_j \frac{\exp\left\{-0.5\left(Tb_o - Tb_s(R_j)\right)^T (O+S)^{-1}\left(Tb_o - Tb_{s(R_j)}\right)\right\}}{\hat{A}} \quad (2)$$

Here, R_j is once again the vector of model profile values from the *a-priori* database model, Tb_o is the set of observed brightness temperatures, $Tb_s(x_j)$ is the corresponding set of brightness temperatures computed from the model profile R_j. The variables *O* and *S* are the observational and model error covariance matrices, respectively, and $\hat{A}$ is a normalization factor. The profile retrieval method is an integral version of the well-known minimum variance solution for obtaining an optimal estimate of geophysical parameters from available information (Lorenc, 1986, for a general discussion).

While the mechanics of Bayesian inversions are fairly well understood, four important issues are discussed separately in the following sections. The first concerns the use of ancillary data to search only appropriate portions of the a-priori database. Previous studies such as Berg et al. (2006) have shown that searching only over the appropriate SST and TCWV over oceans constrains the solution in a significant and positive manner. An important step is, therefore, to select the appropriate *a-priori* profiles in the Bayesian inversion. Rather than perform a retrieval from each sensor, the current algorithm uses ancillary data - Surface Skin Temperature (Tskin) and Total Column Water Vapor (TCWV or TPW) , and Land Surface class. This 3-dimensional classification of the profiles allows for consistency in the a-priori database profile selection

between each of the constellation radiometers. An overview of sources of the ancillary data is discussed in section 3.2, with more details in Section 4.0.

For the Bayesian profile search to succeed, the ancillary data must be added to both the retrieval as well as the a-priori database. Section 3.3 describes the construction of the *a-priori* database itself. Because the databases constructed for each constellation radiometer are based upon the output of the "combined radar/radiometer" algorithm in GPM, it must be noted that that product cannot be used until after the launch of GPM and sufficient time afterwards to generate a robust database. As such, the at-launch algorithm will utilize currently available hydrometeor observations from TRMM, CloudSat, and surface based radars to simulate GPM'S DPR radar.

3.2 A-Priori Profiles – Surface Emissivity Classification

Ancillary data is needed in the algorithm in order to specify the Skin Temperature (Tskin,) Total Column Water Vapor (TCWV) and Surface Type Class in order to classify the a-priori profiles. These parameters are added to each database profile with the highest time resolution available from the input data sources. The output product type and time requirement determine the source of ancillary data to be used. Real-time data needed by the merged products (i.e. IMERGE) requires forecast model output that is available at the time of satellite data collection. The Japanese operational GANAL products (in both forecast and analysis mode) are used for the "real-time" and "standard" products respectively, while the ECMWF ERA-Interim is used for Climate reference Product that requires homogeneous ancillary data over climate time series. As described in section 4, this is handled in the pre-processor portion of the algorithm to minimize changes to the code itself.

A fundamental aspect of the GPM radiometer algorithm is that it has been formulated as an S0, S1 or S2 type retrieval over land. The S0 retrieval assumes no knowledge of the land emissivity and focuses instead of liner channel combinations that are as insensitive to the surface as possible. The S1 retrieval is used when the land surface emissivity, although not well understood, is known to have significant covariance among the channels while the S2 retrieval is used when the surface emissivity is either known or retrievable. Ancillary data is needed to define the surface emissivity classifications and the sections below describe the land surface classifications used in the S1 retrievals, the ocean/land land masks, and the snow cover datasets.

3.2.1 The Land Surface Emissivity Classes

Land Surface Classes are defined as having similar emissivities. As indicated previously, the GPM algorithm is designed to work on an S0 (the surface is not well known), S1 (the surface has unknown but consistent and repeatable emissivity properties) and S2 (the surface emissivity is well understood and predictable using ancillary data). Surface type classification begins with a latitude/longitude classification of land, ocean (or inland water), ice and the three different boundaries that are possible between the three interfaces (land-ocean; land-sea ice and ocean-sea ice). The land classes are further subdivided based upon their mean emissivities. Land surface emissivities have been estimated from all available SSM/I observations from 1993 to 2008, under clear sky conditions (Prigent *et al*. 1997). The dataset has been extensively analyzed and evaluated, by comparisons with both related surface parameters and model outputs. It has been shown to provide robust emissivity calculations, *i.e*., radiative transfer simulations using the

emissivities are closer to the satellite observations. Estimates of the emissivities for all SSM/I frequencies are available with a spatial resolution of 0.25°×0.25° at the equator (equal-area grid) at monthly averaged intervals.

The seven dimensional emissivity space of mean SSMI emissivities has been clustered using a K-means method. The emissivity classes are static but are applied on a monthly basis so that a single point can change classes as a function of time. In Fig. 3, the globe is classified into 10 classes for January (Prigent *et al*. 2008). In this example, class ten is for water-covered pixels, classes 6 to 9 are for snow/ice-covered pixels and classes 1 to 5 are for increasing vegetation cover. Using the TELSEM tool, we have analyzed the correlation structure and the covariance matrices for each class, and each pixel location.

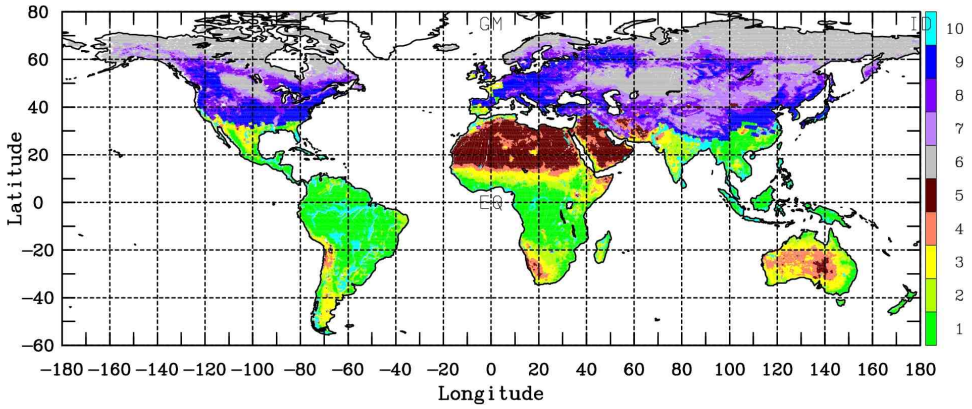

Fig. 3. Clustering of the SSM/I classes in ten self-similar emissivity classes. Ten classes have been defined that correspond to four classes with increasing vegetation, five classes with increasing snow and ice and a class of what appears to be standing water.

For the current version of the algorithm (B2), the classes correspond to self-similar mean emissivities. Subsequent versions will use self-similar co-variances among channels. This change would better fit the GPM post-launch paradigm in that the combined GMI-DPR algorithm that would eventually replace the current algorithm would likely be based upon such a co-variance paradigm were the emissivities could be adjusted to achieve the optimal fit between GMI and DPR.

3.2.2 The Land/Ocean Surface Masks

Sensor specific land masks are created by ingesting the land/sea data from the MODIS/SeaWIFS / Ocean Color land mask (The MOSIS land mask detailed description is given at the following location: http://oceancolor.gsfc.nasa.gov/DOCS/ODPS_Land_Mask.pdf). This was initially generated in 1993 and based on the World Vector Shoreline (WVS) database. This database did not include any inland waterways, so at that time, those areas were simply flagged as land. In October 1997, shortly after the SeaWiFS launch, the file was modified to include inland waterways, based on the World Data Bank (WDB) information. The final result is a 1/128th degree global grid that specifies either land or water. This is the data file from which the GPM land masks are derived. The land mask files are a 1/16th degree grid, derived at two different nominal sensor 19Ghz footprint. If the 1/16th degree grid box doesn't have 100% land or ocean,

the capability to examine finer resolution land/ocean specifications down to 2 km will be made developed and made available.

3.2.3 The Snow Cover Dataset

Retrieved daily from the National Snow and Ice Data Center (NSIDC), are the 4 km Interactive Multi-sensor Snow and Ice Mapping System (IMS) snow cover polar stereographic maps for the northern and southern hemispheres. These data provide a yes/no snow cover that is used to modify the monthly climatology land surface emissivities described in the section above. This modification process is further described in Section 4.

3.3 The *A-Priori* Database

Until the launch of the GPM core satellite, the a-priori database must be put together from existing sources that represent the GPM core satellite capabilities as best as possible. It is done here with sets of matched observations of Tb and an accompanying radar-derived surface rainfall and hydrometeor structure defined as an "observed" dataset. This "observed" dataset could serve as the a-priori database except that there is no direct mechanism to create the same database for the diverse radiometers of the GPM constellation (with slightly different channels, spatial resolutions and view angles). For the latter, a physical model is needed. Each entry in the "observed" dataset is therefore matched to output from a global, one year Cloud Resolving Model (CRM) simulation from the Goddard Cumulus Ensemble model. In this matching procedure, one finds the model profile that most closely matches the observed Tbs and surface rainfall rate, in addition to ancillary fields (TSKIN, TCWV, surface type, T_{2meter} and fractional rain coverage in the radiometer FOV). If there is a good match, the matched CRM profile would have the same Tb and rain as the observed data. Unlike the observed data, however, the CRM pixel has a full physical description of all hydrometeors and can be used to compute the Tb for other radiometers as well. It is therefore the CRM profiles and computed Tb that constitute the core of the a-priori database. It should be noted here, that this is different from earlier versions of the Bayesian algorithm that relied solely on CRM profiles for their a-priori databases. Because of the heavy constraint by the observed Tb and rainfall rates, the CRM plays a much smaller role here than it had in versions that did not constrain the CRM with observations.

3.3.1 The Cloud Resolving Model

The NASA Goddard Multi-scale Modeling Framework (MMF) is based on the coupling of the 2-dimensional Goddard Cumulus Ensemble Model (2DGCE) and the Goddard Earth Observing System (GEOS) GCM. The MMF, which replaces cloud parameterizations with a cloud-resolving model (CRM), is a promising approach in climate modeling, because large-scale cloud parameterization is the largest uncertainties of climate models to project future climate. In other words, MMF takes a hybrid approach to couple low-resolution and high-resolution model physics in a unified framework. The embedded 2DGCEs can explicitly simulate cloud dynamics and microphysics, and provide cloud-precipitation properties and statistics that match the scale of high-resolution satellite observations, while climate model must assume sub-grid horizontal and vertical profiles of these properties. The Goddard MMF includes the GEOS run at 2.5 x 2.0deg (or 1.24x1.0deg) horizontal grid spacing with 32 vertical layers from the surface to 0.4 hPa and a 2D (x-z) GCE embedded at each GEOS column using 64 x 28 (or 32x28 for

1.25x1.0deg case) grid points with 4 km horizontal grid spacing and a cyclic lateral boundary. Globally, there are a total of 13,104 GCEs running at the same time. The time step for the 2D GCE is 10 seconds, and the GEOS-GCE coupling frequency is one hour (i.e. the GEOS physical time step). Because of high MPI scalability, the computational demand of the NASA MMF is far less (1~2 order) than a future global CRM. At each GEOS column, the global model provides the mean atmospheric conditions and the large-scale temperature and moisture advection forcings to the GCE, which feedbacks the tendencies of thermodynamic variables and cloud statistics of a GCM.

Tb is computed for every 1-hr MMF outputs for 12-months period. MMF use 2D GCE simulation (x-y-z =>-64x1x28). For each single column (28layer), Eddingon code was applied to simulated microwave Tb for all frequencies using the GCE microphysics assumption (bulk density, diagnostic size distributions). Surface emissivity is computed from NESDIS land emissivity model that requires several land-surface input parameters. Since this is a collection of 2D GCE simulation, Tb convolution was applied in x-direction only using the AMSR-E cross-tracking IFOV.

A total of 50 million hydrometeor profiles from the CRM were selected based on seasonal and geographical diversity. Using a radiative transfer model with these profiles, T_{bs} at each of the frequency sets of the constellation members were created for these 50 million profiles. For example model frequencies for a TMI match ran from 10 – 89 GHz, while the SSMIS set included frequencies from 18 to 183 GHz. This process also enables us, eventually in the processing, to create the pre-launch database for GMI frequencies. The individual database components discussed next find a subset of these profiles that were observed by each of the sensor combinations.

For completeness, here are the MMF frequency sets for the 3 profile databases:

The frequencies created, for TMI: 10.65, 19.35, 21.3, 37.0, 85.5 GHz, AMSR-E and MHS at 10.65, 18.7, 23.8, 36.5, 89.0, 157.0, 183±7, 183±3, 183±1, 190 GHz, and finally SSMIS at 19.35, 22.235, 37.0, 85.5, 91.0,150.0, 183±7, 183±3,183±1 GHz.

3.3.2 The Individual Database Components

Because there is no single "best" source of an "observed" dataset, the GPM a-priori database is constructed from three distinct sources, each with strengths and weaknesses.

3.3.2a The NMQ and SSMIS dataset

This database was constructed by Nai-Yu Wang from the University of Maryland, ESSIC. It provides the foundation for the land component in the at-launch GPROF2014 database. The observations from DMSP F17 SSMIS brightness temperatures (Tbs) from 19 to 183 GHz microwave channels and NOAA National Mosaic and Multi-Sensor QPE (NMQ) radar derived surface rain-rates are used to produce microwave observations that closely mimic the GPM GMI. This observed SSMIS Tbs and NOAA NMQ rain rates were paired with profiles from the GSFC Goddard Multi-scale Modeling Framework (MMF) to produce the vertical hydrometeor profiles, microwave T_{bs}, and surface rain rate as described above. This semi-physical database has the

advantage of combining observed Tb and rain rates with profiles that reproduce the right Tb and surface rain and can therefore also be used to generate the radiometer constellation databases.

The generation of this database can be thought of a two-step processes : (1) 0.01 deg (~1km) NMQ surface rain-rates are beam-averaged to SSMIS 37 GHz field of view (FOV, ~27 Km X 45 km) to produce combined SSMIS/NMQ Tbs/surface rain-rate observations (2) selecting GSFC MMF/CRM model simulations that match with SSMIS/NMQ observations to get the complete vertical hydrometeor profiles that closely matched Tbs/rain-rate observations for the purpose of applying the database to all constellation radiometers.

One year of F17 SSMIS observed TBs and NMQ rain-rates from December 2009 to November 2010 are used to generate the observational database. The 1-km NMQ rain-rates are convolved to the SSMIS 37 GHz FOV based on a two-dimensional Gaussian antenna beam pattern g

$$g = \exp\left[-\left(\left(\frac{X}{FWHMX}\right)^2 + \left(\frac{Y}{FWHMY}\right)^2\right) \times 4 \times \ln 2\right] \qquad (1)$$

Where FWHMX (27km) and FWHMY (45km) are the full width at half maximum at along track and cross track directions, respectively. The DMSP satellite altitude is assumed constant at 833 km. Figure 4 shows an example of the original NMQ 1km resolution and SSMIS 27km x 45 km beam-averaged rain-rates .

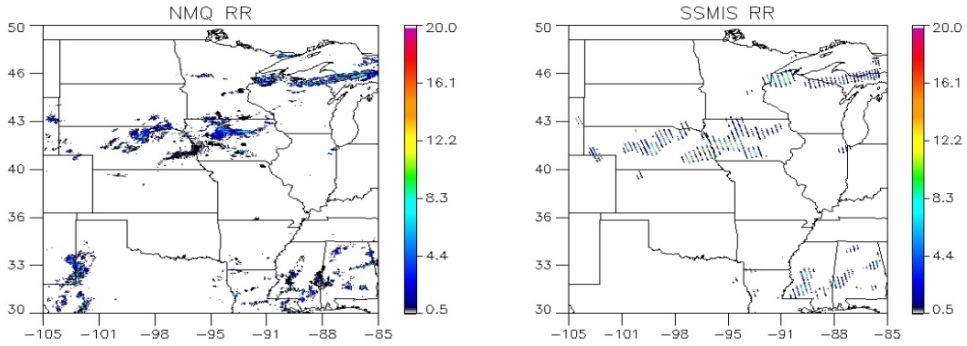

(a) (b)

Figure 4. Surface rain-rates from June 1, 2010 from (a) NOAA radar composites NMQ at 1 km resolution (b) same NMQ rain-rates convolved to SSMIS 37 GHz footprint area of 27 km by 45 km

The SSMIS/NMQ observational database contains entries include the following observations

$$\bar{y} = \begin{bmatrix} Tb19_{V,H} \\ Tb22_{V} \\ Tb37_{V,H} \\ Tb91_{V,H} \\ Tb150_{H} \\ Tb183 \pm 6_{H} \\ Tb183 \pm 3_{H} \\ Tb183 \pm 1_{H} \\ T_{2m} \\ RR \\ rain\_frac \end{bmatrix} \qquad (2)$$

where the *TbXX* entries indicate various SSMIS radiometer channels with vertical (*V*) and/or horizontal polarization (*H*) capabilities, T_{2m} is the 2-m temperature, *RR* the NMQ-derived surface precipitation rate, and *Rain_frac* the fraction of rain determined from NMQ ground radars within the approximate radiometer footprint.

Both observational and modeling datasets are binned by skin temperature (1 K bins), total precipitable water (1 mm bins), and surface emissivity class. Each MMF model profile and associated MMF/SDSU simulated Tb combination is then optimally matched with an observational profile from a similar skin temperature/total precipitable water/surface emissivity class bin. Observational profiles are searched for within +/- 2 mm total precipitable water and +/- 4 K skin temperature bins over land. The best modeling profile match for a given observational profile is computed using a distance minimization technique, where the distance, *D*, between observation and modeling space is calculated by the following formula:

$$D = \sqrt{D_{Tb}^2 + D_R^2 + D_{FL}^2 + D_{FOVCover}^2} \qquad (3)$$

Where the total distance *D* is the sum of distances from Tb, rain rate, freezing level (using the 2m temperature as the proxy), and the fraction of rain within the satellite radiometer FOV. The D_{TB} is the difference between simulated and observed brightness temperature, defined by:

$$D_{Tb} = \sqrt{\frac{1}{Nchan} \sum_{i=1}^{Nchan} \left(\frac{Tb_{i,mmf} - Tb_{i,obs}}{\sigma_i} \right)^2} \qquad (4)$$

where N_{chan} is 11 and represents the number of SSMIS channels included in the datasets listed in eq (2), TB_{mmf} and TB_{obs} are the respective modeled and observed brightness temperatures for each frequency, and σ_i is the frequency-dependent combined observational and modeled uncertainty ranging from fairly low magnitudes of 3 K for the SSMIS 22V channel to much higher values of 14 K for the scattering-sensitive 150 GHz channel.

The other terms in the distance equation similarly represent differences between model output and observations represented in eq (4). The uncertainty σ_i for 2-m temperature difference

term D_{FL} is assumed to be 5K. The uncertainty σ_i for precipitation rate difference term is directly related to the rainrate defined by $0.25R^{0.75}$. The D_{FOV} is not included in the modeling database and is not part of the distance calculation at this time.

The above finds the best profile for the a-priori database for SSMIS for all Ts, TPW and emissivity classes covered by the SSMIS orbit over a year. Figure 5 shows the distribution of the final MMF-SSMIS matched database in each of the surface emissivity class, plotted as a function of surface temperature Ts and total water vapor TPW.

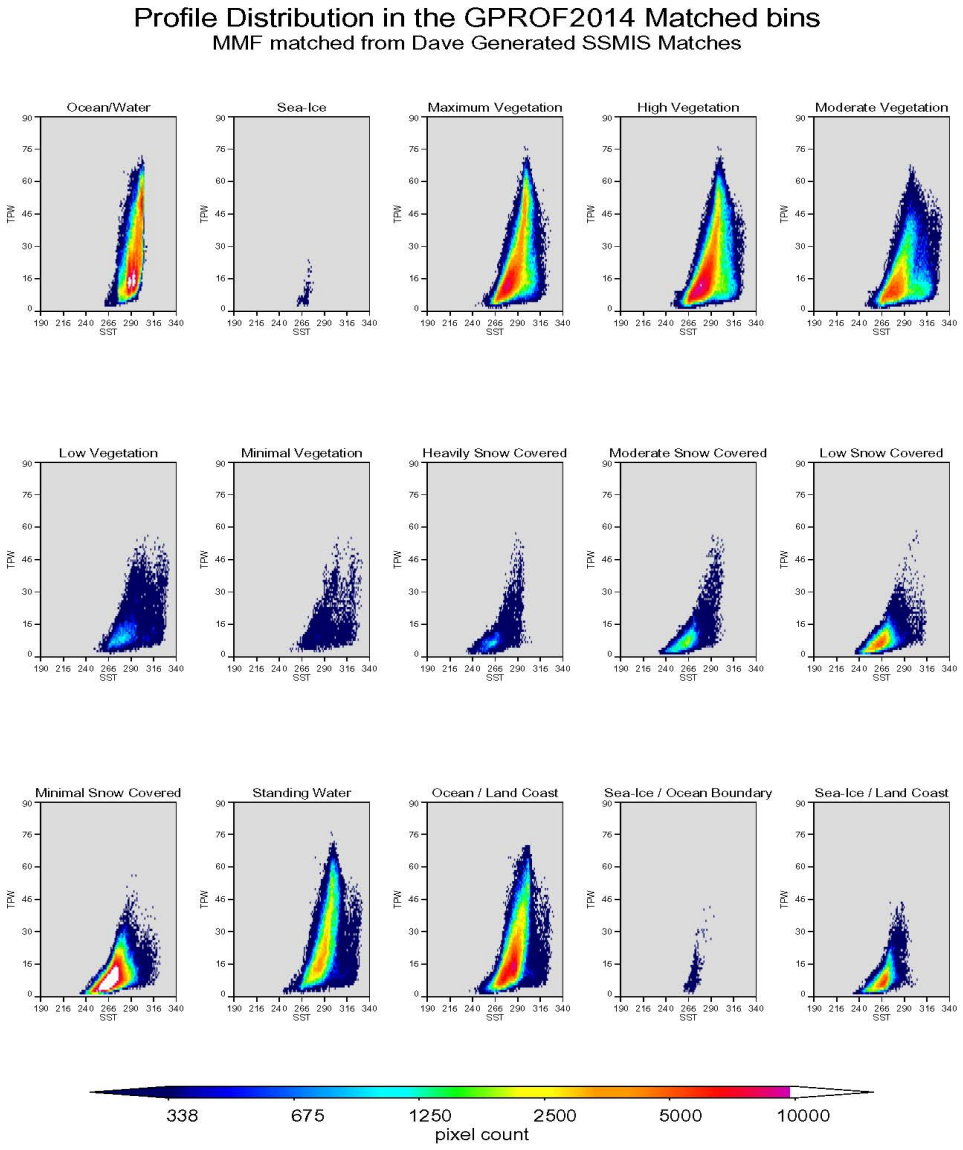

Figure 5. The distribution of the final MMF-SSMIS matched database in each of the surface emissivity class, plotted as a function of surface temperature Ts and total water vapor TPW.

3.3.2b The PR and TMI Dataset

This second observational database used TRMM PR with coincident TMI, and was constructed by Sarah Ringerud and David Randel at Colorado State University. It provides majority of a-priori profiles in the tropics from 38ºN to 38ºS. This dataset had already been used successfully in TRMM retrievals. It's major shortcoming for GPM are geographical limitation of the profiles, thus producing few profiles of cold surface temperatures and associated TCWV amounts. It does however, cover the tropical land and ocean masses exceedingly well and uses frequencies from 10 – 85 GHz.

To match the PR with TMI, a subset of eleven pixels in the center of the PR swath and the nearest TMI matched footprints define the area used for database construction. One year of coincident observations were used from July 1999 – June 2000 and PR Rainrates were convolved to the 37 and 19 GHz footprints, though only the 37 GHz were used to match with the MMF profiles. The matching procedure with the MMF used identical parameters as the SSMI/NMQ and AMSR-E/MHS / Cloudsat . The set of TMI Tbs uses the forward model channel errors to supply the channel weighting matching procedure. The other parameters include the rain rates, 2 meter temperature, and fractional amount of raining PR pixels within the TMI footprint. The profiles were also sub-setted or binned into self-similar groups of TCWV/TSKIN/Surface Class. As in the NMQ/SSMIS the matching vector minimizes the difference of the MMF parameters with the observed values:

$$\bar{y} = \begin{bmatrix} Tb10_{V,H} \\ Tb19_{V,H} \\ Tb22_{V} \\ Tb37_{V,H} \\ Tb85_{V,H} \\ T_{2m} \\ RainRate \\ rain_{frac} \end{bmatrix}$$

The search parameters for the 'best' or closest MMF were also, as in the other profile matching datasets, restricted to profiles within identical TCWV / TSKIN / Surface Classifications bins.

3.3.2c The CloudSat and AMSR-E/MHS dataset

The CloudSat and AMSR-E/MHS profiles were created by Mark Kulie at the University of Wisconsin. Collocated observations from A-Train satellite constellation members CloudSat and AMSR-E provide the foundation for one component of the GPROF 2014 extra-tropical radar-radiometer empirical dataset. Furthermore, higher frequency observations from the Microwave Humidity Sounder (MHS) are also used to complement AMSR-E to produce an observational microwave channel combination that is intended to resemble the GPM Microwave Imager (GMI) channel selection. A multi-year (2006-2010) dataset of near-coincident CloudSat, AMSR-E, and MHS observations is used to generate a candidate merged dataset containing over 160 million space borne radar-radiometer observations that captures a diverse set of extra-tropical locations

and weather conditions. This observational dataset is used to find simulated atmospheric profiles with very similar rain rate and Tb in the Goddard Multi-scale Modeling Framework (MMF). Further details of the observational dataset generation and numerical model output matching process are outlined below.

An observational data vector is built for each coincident CloudSat/AMSR-E/MHS dataset entry makes use of some unique reflectivity information available from CloudSat while also guarding against use of CloudSat inferred rain in heavy rainfall situations. This makes construction of the precipitation profiles somewhat different than the other two data sets.

The CloudSat/AMSR-E/MHS observational vector contains the following elements:

$$\vec{y} = \left\{ \begin{array}{c} T_B 10_{V/H} \\ T_B 18_{V/H} \\ T_B 23_{V/H} \\ T_B 36_{V/H} \\ T_B 89_{V/H} \\ T_B 157 \\ T_B 183.3 \pm 1 \\ T_B 183.3 \pm 3 \\ T_B 190.3 \\ T_{2m} \\ R \\ PIA \\ Z_e PC_1 \\ Z_e PC_2 \\ Z_e PC_3 \\ Z_e PC_4 \end{array} \right\}.$$

Descriptions of the CloudSat/AMSR-E/MHS observational vector elements follow:

$T_B XX_{V/H}$: AMSR-E brightness temperatures at the 36 GHz footprint resolution. AMSR-E 6 GHz observations are not used in this dataset.

$T_B XX$: MHS brightness temperatures at native resolution. Unlike the conically scanning AMSR-E, the MHS is a cross-track scanning instrument with varying observation angles. MHS observations included in this extra-tropical dataset, however, contain primarily low-angle observations. Fig. 6 illustrates the relative frequency of MHS scan angles for the entire dataset.

T_{2m}: 2-m temperature from the CloudSat ECMWF-AUX product.

R: CloudSat-derived near-surface precipitation rate. Rain/snow partitioning is performed using the ECMWF 2-m temperature. If the 2-m temperature is 0°C or below, solid precipitation is assumed and the $Z = 21.6S^{1.2}$ reflectivity to snowfall rate (*Z*-*S*) relationship is used to obtain the liquid-equivalent precipitation rate from near-surface

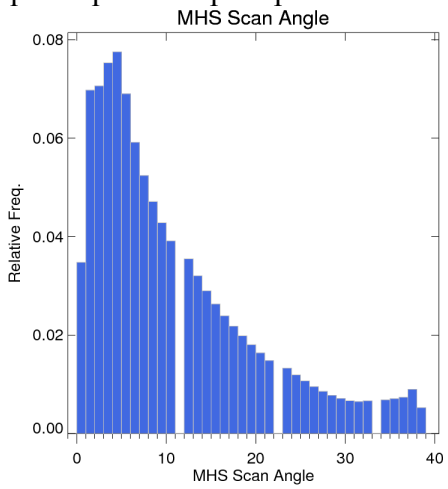

Figure 6. Relative Frequency of MHS scan angle.

CloudSat reflectivity observations (Hiley et al. 2011). For precipitating CloudSat observations associated with above-freezing temperatures, rainfall rates from the CloudSat 2C-PRECIP-COLUMN product are used over ocean. Over land, rainfall rates are obtained directly from near-surface reflectivity CloudSat observations using the rainrate-dependent 94 GHz *Z*-*R* relationships from L'Ecuyer and Stephens (2002), where $Z=29.2R^{0.71}$ if R is less than 11 mm h^{-1}, or $Z=42.2R^{0.55}$ if R exceeds 11 mm h^{-1}. Precipitation rates are convolved to the approximate AMSR-E 36 GHz footprint size.

PIA: W-band path integrated attenuation (PIA) from the CloudSat 2C-PRECIP-COLUMN product, convolved to the approximate AMSR-E 36 GHz footprint size. This field is not included in other observational datasets.

Z_ePC_{1-4}: Four significant principal components (PC) derived from a principal component analysis (PCA) of CloudSat reflectivity profiles associated with near-surface precipitation. The PCA is performed for each 2-m temperature bin (3K bin increments) and CloudSat echo top height associated with precipitating observations. The same PCA is performed for the MMF/SDSU simulated reflectivity profiles. The PCs are used in the observation-modeling matching procedure and are considered preferable to matching simulated versus observed reflectivity fields to minimize differences due to potentially biased ice model scattering properties used to calculate simulated W-band radar reflectivity fields. These fields are not included in other observational datasets.

Note that rain fraction is not used in the CloudSat/AMSR-E/MHS database since the CloudSat swath inherently cannot provide a robust estimate of the total rain fraction within the radiometer footprint.

MMF/SDSU model output are also a critical component of the empirical extratropical dataset, and corresponding "model vectors" comprised of similar elements as the CloudSat/AMSR-E/MHS observational vector are produced globally. The modeled MHS brightness temperatures are simulated at five discrete scan angles (0.0, 21.0, 29.0, 34.0, 38.0 degrees from nadir) and are interpolated to the actual observed MHS scan angle in the observation-model matching process described below. Both observational and modeling datasets are binned by skin temperature (1 K bins), total precipitable water (1 mm bins), and surface emissivity class, then each model profile and associated MMF/SDSU simulated brightness temperature/radar reflectivity combination is optimally matched with an observational profile from a similar skin temperature/total precipitable water/surface emissivity class bin. Observational profiles are searched for within +/- 2 mm total precipitable water and +/- 2 (4) K skin temperature bins over ocean (land). The best observation match for a given model profile is computed using a distance minimization technique, where the distance, *D*, between observation and modeling space is calculated by the following formula:

$$D = \sqrt{D_{TB} + D_{T2m} + D_R + D_{PIA} + D_{PC1} + D_{PC2} + D_{PC3} + D_{PC4}} \ ,$$

where D_{TB} is the difference between simulated and observed brightness temperature, defined by:

$$D_{TB} = \sqrt{\frac{1}{Nchan}\sum_{i=1}^{Nchan}\left(\frac{TB_{i,MMF} - TB_{i,obs}}{\sigma_i}\right)^2} \ ,$$

where N_{chan} equals 14 and represents the total combined number of AMSR-E/MHS channels included in the datasets, TB_{MMF} and TB_{OBS} are the respective modeled and observed brightness temperatures for each frequency, and σ_i is the frequency-dependent combined observational and modeled uncertainty ranging from fairly low magnitudes (2 K) for the AMSR-E 10H channel to much higher values (15 K) for the scattering-sensitive 157 GHz channel. The frequency-dependent uncertainties for the AMSR-E/MHS channels are defined to mimic the SSMIS uncertainties at similar frequencies.

The other terms in the distance equation similarly represent differences between model output and observations. For instance, the 2-m temperature difference term, D_{T2m} , is written as:

$$D_{T2m} = \sqrt{\left(\frac{T_{2m,MMF} - T_{2m,OBS}}{\sigma_{T2m}}\right)^2} \ ,$$

where σ_{T2m} is assumed to be 5K.

The precipitation rate difference term, D_R, is as follows:

$$D_R = \sqrt{\left(\frac{R_{MMF} - R_{OBS}}{\sigma_R}\right)^2} \ ,$$

where σ_R weights the model-observations differences and is directly related to the rainrate:

$$\sigma_R = 0.25 * R_{OBS}^{0.75}.$$

The path integrated attenuation difference term, D_{PIA}, is written in similar fashion as:

$$D_{PIA} = \sqrt{\left(\frac{PIA_{MMF} - PIA_{OBS}}{\sigma_{PIA}} \right)^2},$$

where σ_{PIA} is assumed to be 7 dB and reflects potentially large uncertainties due to ice model scattering properties that may affect simulated W-band attenuation values.

Finally, the reflectivity principal component terms, $D_{PC1\text{-}4}$, are as follows:

$$D_{PIA} = \sqrt{\left(PC_{i,MMF} - PC_{i,OBS} \right)^2}$$

The PIA and surface rainrate terms are only considered for precipitation rates below 5 mm h^{-1} to avoid W-band attenuation and/or multiple scattering complications. Therefore, if surface precipitation rates exceed 5 mm h^{-1}, the matching formula only considers brightness temperatures, 2-m temperatures, and PC fields. However, excessive rainfall rates comprise only a small percentage of the extratropical database entries (Fig. 7) and these restrictions are not frequently utilized. Furthermore, the PIA term is ignored over land surfaces since CloudSat PIA is calculated only over oceans using the surface reference technique.

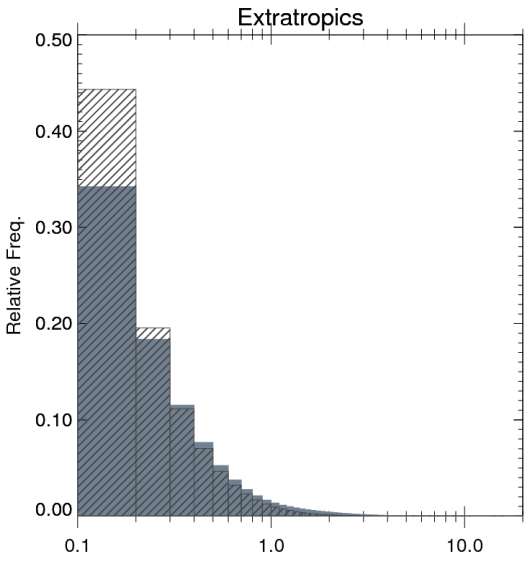

Figure 7. Relative Frequency of CloudSat derived precipitation rates (gray) and MMF precipitation rates (hatched).

After a match has been identified by minimizing the distance between the model output and observations, the microphysical profile and model-derived precipitation rate for each observation is retained in the database.

3.3.2d Cross-Track Scanners AMSU-B and MHS

The Cross-track database creation and code development is under control of Chris Kidd. The difficulty is the EIA changes with each of the 90 scan angles. Databases for a prescribed number of angles are being created and tested. Interpolation of the Tbs between the angles is the most likely method of reducing the number of complete databases for each angle to a manageable number. Chris Kidd (personal communication) expects to complete a test version of the algorithm and databases for the B3 release of the Algorithm, June 30th, 2013.

3.3.3 Pre-launch Profile Database

The following description speaks to Figure 8, the flow diagram of pre-launch database creation:

The entire left side of the figure up to and including the "Match Sat Obs profile" box was performed for each of the 3 hydrometeor / brightness temperature datasets described in the previous sections. The result of these matching processes was an output of the best-matched profile written into a "MMF profile list". At this point each bin was populated with a maximum of 10,000 observed profiles. We believe that 10,000 profiles per bin should provide enough diversity to meet retrieval requirements.

The difference between the T_b observed and T_b (MMF/CRM) is then calculated for each chosen profile for three application steps. The first is to calculate the mean T_b offsets for each channel and for each surface type so that later we can remove this T_b bias from the CRM T_{bs} when comparing the T_{bs} in the GPROF2014 Bayesian retrieval. Second, this average difference information is also used in GPROF2014 to define the channel sensitivity weights. Finally, the T_b biases are used in the creation of the channel reduction coefficients for the S0 retrieval.

The final step merges the three observational datasets selecting profiles from the MMF/CRM profiles in each 3-dimensional bin, 'filling' up to a bin maximum of 10,000 profiles. The profiles can be selected from any of the MMF/CRM sensor specific datasets since they all have identical profile counts in the daily gridded files. The logic to selecting profiles between the 3 observational dataset is as follows: The SSMIS/NMQ matched profiles are used first and if more than 10,000 profiles are available, a subset of 10,000 is chosen randomly. If a bin is filled, no additional profiles are added. If a bin is not filled, the TMI/PR matched profiles are next used up to 10,000 profiles in a bin. A random subset of TMI/PR profiles is again used to reach the bin maximum. Finally if the profile count in the bin still is less than 10,000, the procedure is repeated, adding additional matched profiles from CloudSat/AMSRE/MHS. At this point, the sensor profile database is complete with a maximum of 10,000 matched CRM profiles per bin. The complete profile list can be used to pull the a set of database profiles from ANY of the MMF/RT files and can therefore be used to create a pre-launch database using any of the input frequency datasets, including those matching GMI.

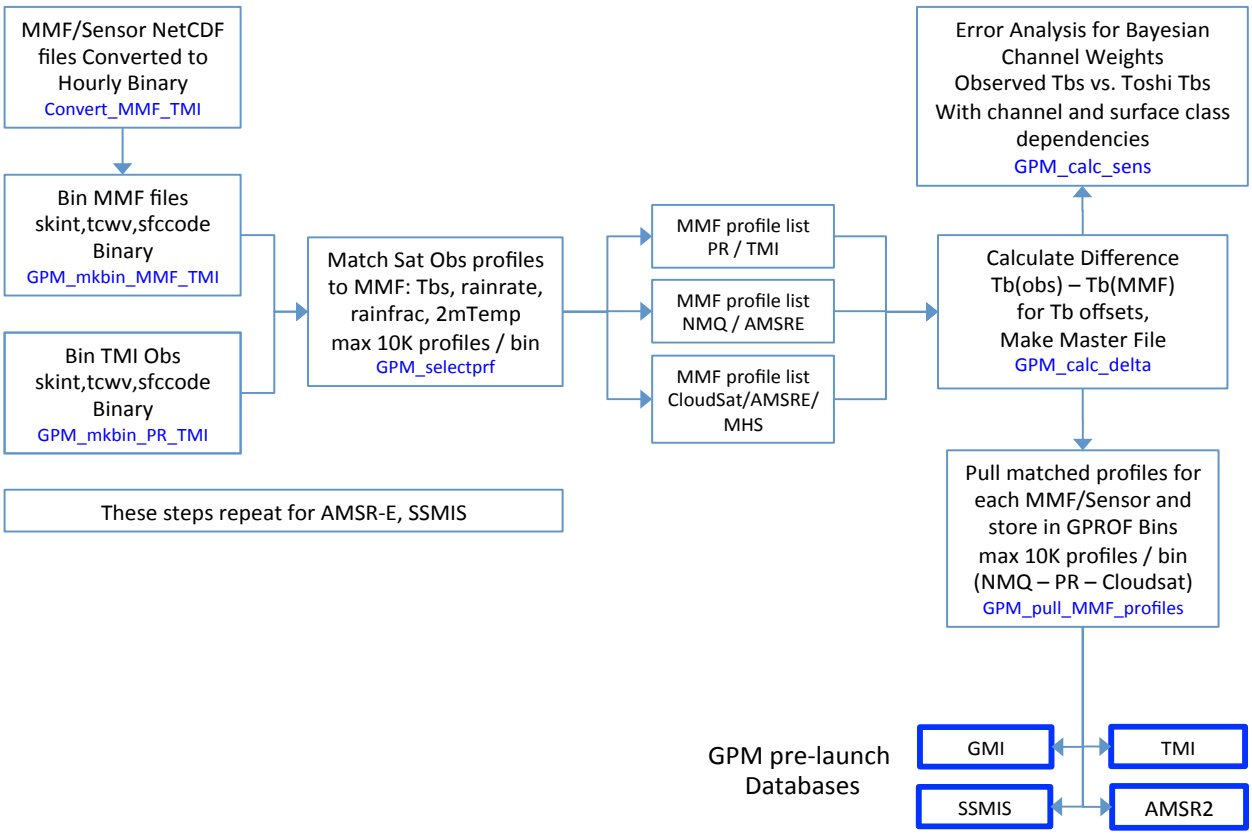

Figure 8. The GPM Pre-Launch Database Creation Process

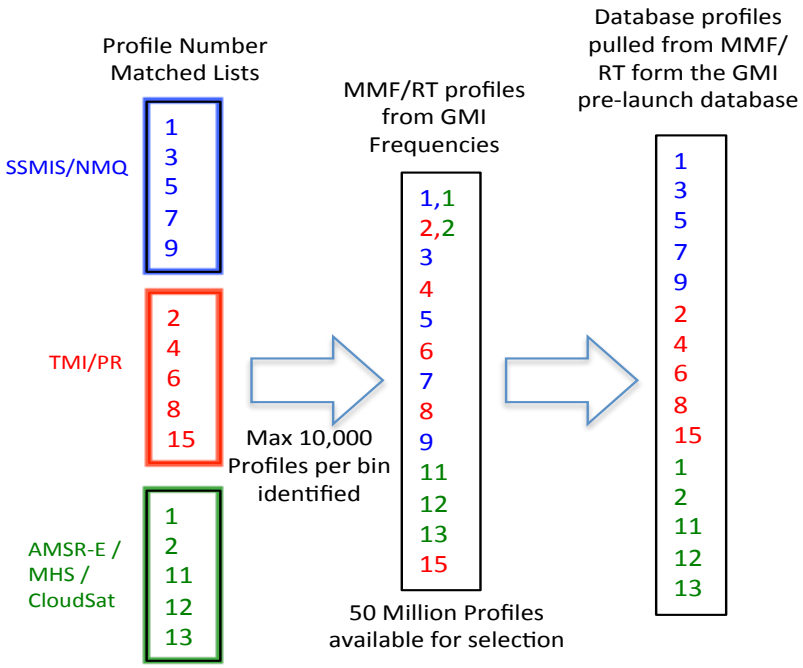

Figure 9. Profile Selection for the Pre-launch GMI database.

3.4 Channel Uncertainties

Uncertainties in physical inversions come from a combination of sensor noise and forward assumptions and errors. As described in Stephens and Kummerow (2010), rainfall retrieval errors tend to be dominated by the forward model assumptions. That is the case here as well and is particularly true when surface characteristics are not well known.

In the S1 and S2 solutions, the uncertainty is determined from the fit between the observed dataset and the CRM T_b that ultimately make the a-priori database. The computed uncertainties, organized by surface code and satellite frequency computed using TMI, SSMI, SSMIS and AMSR-E are presented in Table 5.

For the S0 solution, a EOF analysis is performed to select liner combinations of channels that are insensitive to the surface. In this scheme, the EOF are normalized and channel uncertainty is given as 1 unit.

Table 5. Computed Channel Uncertainties for all Surface Types

sfctype	10V	10H	19V	19H	22V	22H	37V	37H	89V	89H	150V/H	183/7	183/3	183/1
1	4.226	4.583	3.256	4.452	2.693	3.105	3.142	5.636	3.612	7.029	5.135	4.053	3.203	3.242
2	2.772	3.772	3.065	3.399	2.994	3.163	3.684	4.646	5.270	6.051	**5.960**	**4.210**	**3.260**	**3.220**
3	5.570	7.208	3.679	4.813	2.634	2.115	2.557	3.828	2.902	4.335	3.778	3.259	2.558	2.664
4	5.515	6.763	2.928	3.895	2.201	2.470	2.233	3.765	2.778	4.255	3.850	3.343	2.652	2.768
5	5.636	6.311	3.947	5.139	2.941	2.908	2.771	4.429	2.977	4.249	3.749	3.434	2.726	2.934
6	5.782	6.700	5.859	7.089	4.443	3.380	3.924	5.677	3.699	4.811	3.668	3.699	2.987	3.265
7	6.036	6.882	6.866	7.538	5.028	3.455	4.251	5.499	3.662	4.348	4.651	4.124	3.473	3.719
8	2.972	4.204	3.243	4.200	2.889	3.718	3.756	4.984	5.287	5.761	5.957	4.206	3.263	3.223
9	3.571	4.664	3.576	4.365	3.166	3.597	3.731	4.826	4.929	5.406	5.629	4.157	3.306	3.225
10	3.307	4.308	2.605	3.706	2.272	3.150	3.279	4.511	4.514	5.113	5.996	4.056	3.005	3.054
11	3.105	3.980	1.905	2.895	1.524	2.407	2.333	3.852	3.371	4.562	5.448	3.663	2.652	2.713
12	5.126	6.731	3.823	5.456	2.739	3.090	2.743	4.460	3.146	4.586	3.981	3.587	2.917	3.070
13	6.255	9.623	4.732	6.975	3.539	**4.000**	3.501	6.954	4.207	8.407	6.023	4.084	3.504	3.719
14	**7.321**	**8.079**	**1.657**	**2.794**	**1.205**	**2.000**	**2.537**	**5.441**	**3.826**	**6.603**	**6.351**	**3.756**	**2.978**	**3.088**
15	7.321	8.079	1.657	2.794	1.205	**2.000**	2.537	5.441	3.826	6.603	6.351	3.756	2.978	3.088

Estimated values for Version B2 are highlighted in **Yellow.** The estimated valued are limitations of the version B2 implementation in the surface classes and will be significantly reduced or eliminated in version B3.

The surface types are: 1 = ocean/water, 2 = sea-ice, 3-7 = decreasing vegetation, 8-11 = decreasing snow cover, 12 = standing water/rivers, 13,14,15 = coastlines and sea-ice boundaries.

4.0 ALGORITHM IMPLEMENTATION

The code to ingest T_bs and ancillary files, perform quality control, assign surface types and decide on channel selection will be written and maintained at Colorado State University in Fort Collins, Colorado, USA. The architecture will be open to all team members as well as outside parties. We will use the input and output sections of this ATBD as a living document that is intended not only for the user of the precipitation product, but also for the algorithm developers to convey precise information about procedures, methods and formats. The code will strive to be machine independent but will first order everyone on the algorithm development team to match the architecture planned by the PPS.

The algorithm itself consists of Fortran 90 code that's self-contained in the Algorithm directory. All parameter fields and static databases must be accessible from this directory location as well as the dynamic ancillary data fields. These include the daily SST and sea-ice fields read in from NOAA's Reynolds high-resolution analysis (Reynolds *et al.* 2006) and the various atmospheric background fields read in from the GANAL and ECMWF analyses.

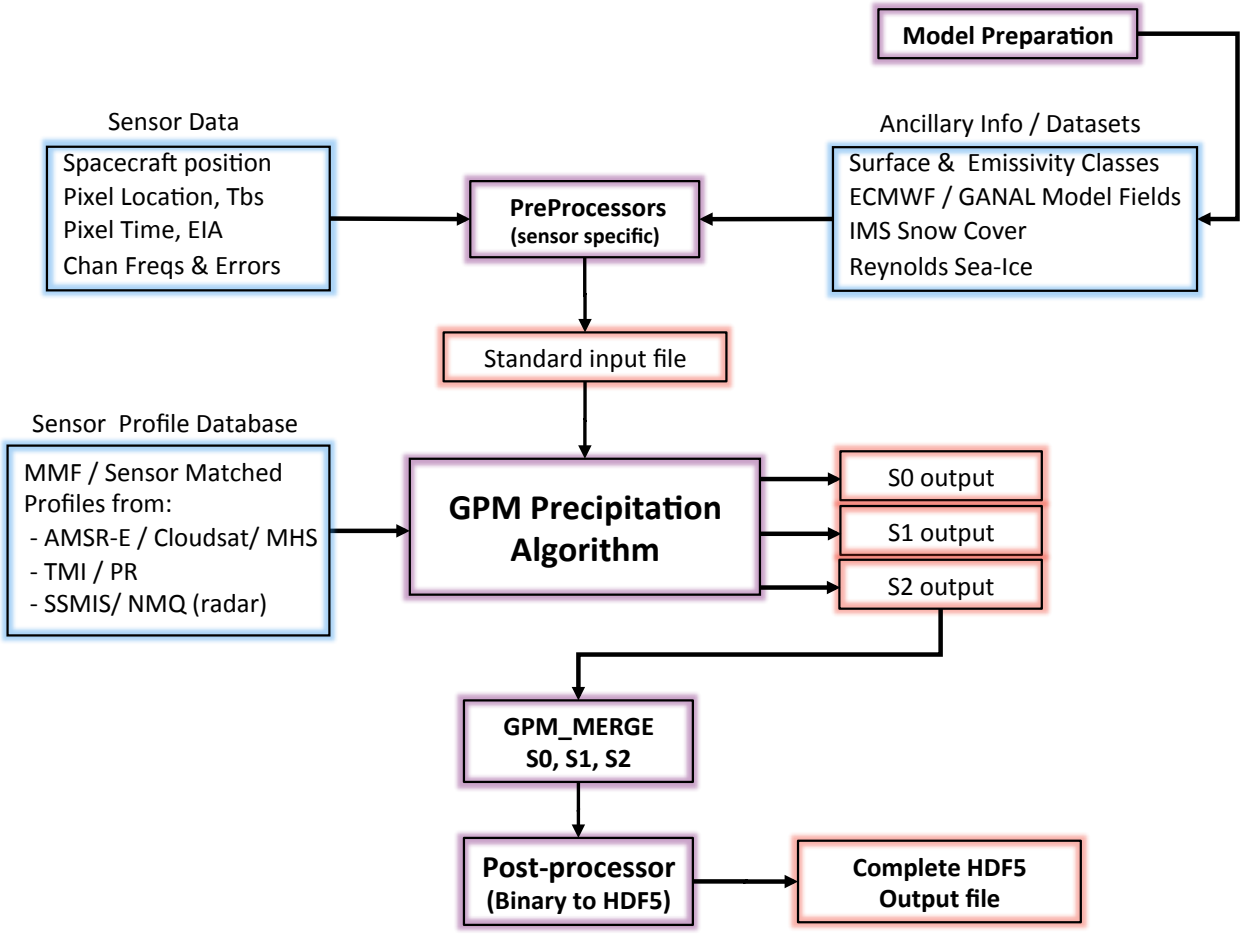

Figure 9. Overview of the processing steps for the GPM Precipitation Algorithm.

Five processes (Figure 9 in the purple boxes) are to be run at the PPS to complete the Radiometer Precipitation Algorithm (PA). The following is a description of each.

4.1. Model Preparation

The model preparation process ingests both the GANAL and ECMWF GRIB formatted files. The files are unpacked into simple binary grids and any additional parameters needed by the preprocessor (e.g. GANAL TCWV from a profile of relative humidity) are computed. Other data processing includes the Orographic Lifting Index, and time interpolation between the 6 hourly model times to up to hourly fields. Output is to a multi-parameter structure of all variables needed by GPM PA at each model grid point. This model prep routine can be modified easily for additional parameters that might be specified in the future.

For real-time and near real-time GPROF2014, the JMA GANAL global model fields will be used. These can be retrieved from the JMA to JAXA to the PPS data flow very shortly after the analysis time. Parameters retrieved will be at the surface: surface pressure, MSL pressure, U and V component winds at 10 meters. 2 meter temperature. 2 meter relative humidity, and Skin Temperature. The vertical profiles on constant pressure surfaces are: Temperature, Vertical Velocity, U and V component winds, relative humidity, and geopotential height (the actual altitude of the pressure surfaces). Model data is assimilated every 6 hours for both profile and surface. The spatial resolution of the GANAL global grids is 0.5 X 0.5 degrees.

Approximately 2 months past real-time the ECMWF interim re-analyses are available. The following data fields will be downloaded and used for the GPROF2014 Climatological processing: 2 meter Temperature, 2 meter dew point, total column water vapor, surface pressure, and Skin Temperature. Also there are vertical profiles of Temperature, U and V component winds, specific humidity, and geopotential height (the actual altitude of the pressure surfaces). Model data is assimilated every 6 hours for both profile and surface, and a 3-hour forecast is available for the surface parameters.

4.2 GPM Preprocessors

The preprocessor is the interface between the orbital data files (L1C format) and the GPM PA. The GPM sensor specific preprocessor reads from the L1C HDF files and creates the standard input file format. The preprocessor assigns all the ancillary data to each observed pixel along with the pixel's T_{bs}, latitude/longitudes, and sensor specifications. Also here in the preprocessor, the surface emissivity classes, the land masks, the daily Reynolds sst/sea-ice (downloaded once per day from NCDC), and model 2-meter surface temperature are used to create a surface classification for each pixel. Within the surface classification procedure, the IMS snow cover data is ingested and is used to modify the monthly climatological surface emissivity classes in the following way. If the emissivity classification says there is snow cover, but the IMS says 'no', we query previous months surface emissivity classes to find the last surface class when there was not snow. This process might repeat for 6 previous months until a 'without snow cover' emissivity class is found. Alternately, the emissivity class might say 'no snow on ground'

but the IMS snow has snow cover. In this case we change the emissivity class to the lowest level of snow cover – minimal snow.

Other parameters are also output from the preprocessor including the names and locations of the ancillary data directories, and profile databases - everything the GPM PA needs to run the rainfall retrievals. The complete description of the preprocessor output parameters of the is given in Appendix B.1.

4.3 GPM Precipitation Algorithm – GPROF2014

The GPM Precipitation Algorithm (GPROF2014) starts by reading the Standard Input file produced from the preprocessor. This includes all the ancillary data needed to match the SkinTemp/TCWV/SurfaceClass in the profile databases. These 3-dimensional matching is used to subset the entire set of database profiles for the Bayesian precipitation and profile retrieval. As a final step, the profiles of each of the hydrometeor species are best matched to a database of 2100 representative profiles for each species. This step reduces the data volume of the output files. The output is to a native binary formatted file. The description of the output parameters from the GPROF2014 is given in Appendix B.2.

4.4 GPM Merge

As was explained earlier, the GPROF2014 can run 3 different versions – S0 where the surface emissivity is unknown; S1, where the know something of the surface, but it might only be a climatology; and S2, where the surface emissivity is dynamic and well described. We expect that there will always be at least two of these versions executed for each pixel. The GPM Merge routine will combine these individual runs into a single output product. At present for Version B2, we imply insert the S0 retrieval in the S1 whenever there is one of 3 coastal surface classes. The resultant output file always includes a flag for which retrieval was used for each orbital pixel. The parameter list is identical to that from the GPROF2014 Precipitation Algorithm.

4.5 GPM Post-Processor

The GPM Post-processor reads the native binary output from the GPM Merge routine, attaches additional metadata from the original orbital L1C file and writes out a final HDF5 formatted GPM GPROF2014 file. The steps described above are graphically represented in the Figure 4 :

5. ALGORITHM TESTING, VALIDATION, and RESULTS

5.1 Version B2 Software Distribution

The Science version B2 of the Precipitation Algorithm is available for testing by the science team. The distribution is available at Colorado State University via anonymous FTP download.

ANONYMOUS FTP INSTRUCTIONS
---
ftp rain.atmos.colostate.edu
anonymous login
cd pub/GPM
ascii
get AAREADME
bin
get GPM_05012013.tar.gz

Four sets of preprocessor files are available within the /preprocess/ subdirectory. First, there are two months (January 2012, and September 2012) of preprocessor files for SSMIS F17. Second, there are 2 sets of (including F16, F17, F18) orbits for times when an SSMIS overpass occurs over the GCPEX and MC3E field projects. The AAREADME file describes the folders and other information for the Version B2 distribution. Also included are folders with the GPM Precipitation Retrieval Code (GPROF2014), and IDL and Fortran read routines to read the binary output format. The ancillary files necessary to create the preprocessor files are quite voluminous since they include the ECMWF, Reynolds SST, and others. We can easily create additional preprocessor files upon request (reasonable requests!) and this will still be easier than supplying the entire many years of ancillary files. However, for selected users we might also prepare a subset of the ancillary files necessary to run the preprocessor on user selected times periods, although these will be strictly limited due to their data volume.

5.2 Algorithm Results

The following figure (Figure 10) show the ascending and descending orbit sections for 14 orbits from SSMIS/F17 for January 3rd, 2012. These orbits are in the software distribution, and the script files necessary to create them are in the S0S1_B2 (the GPROF2014) folder.

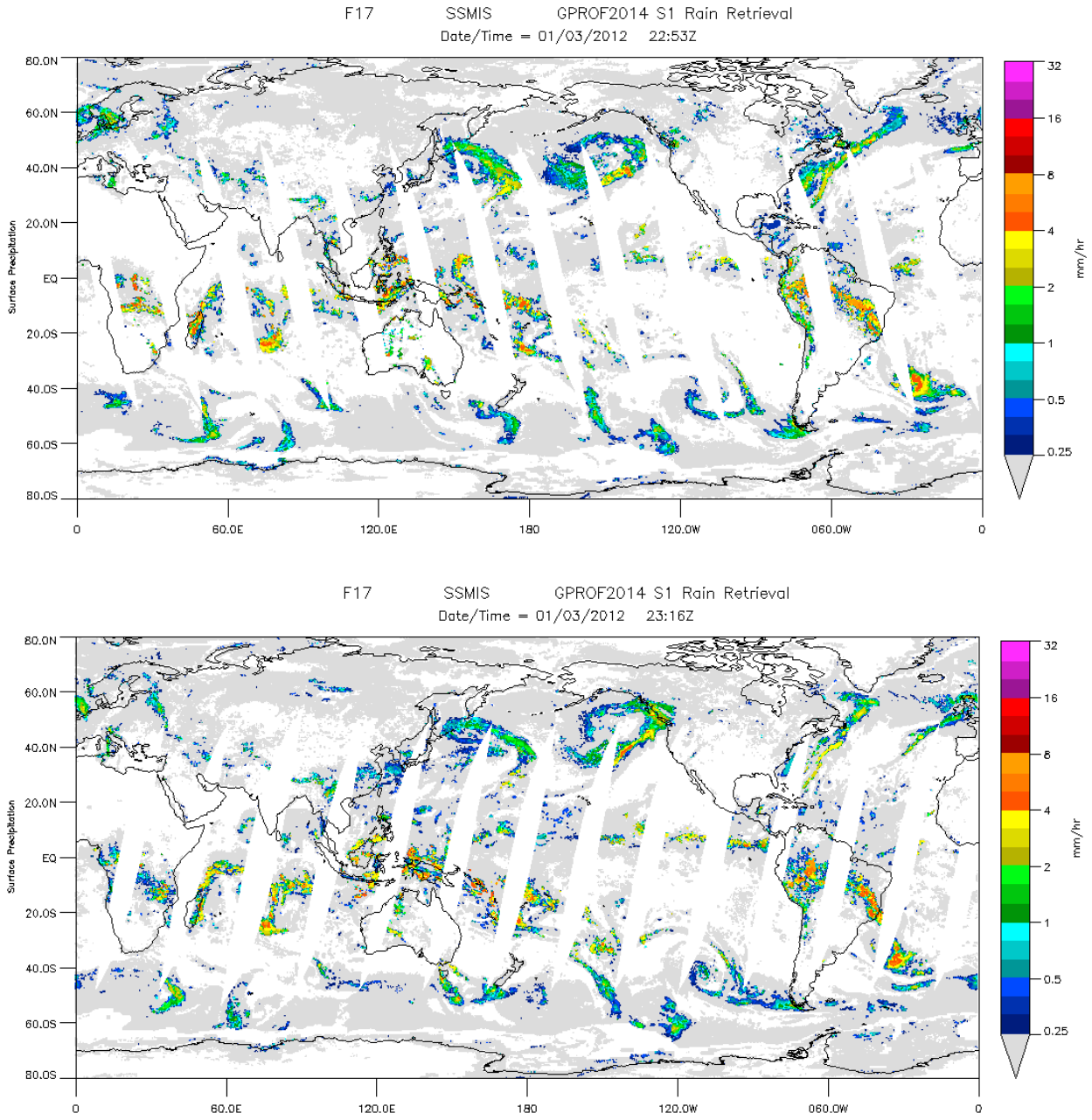

Figure 10. January 3,2012 ascending and descending orbit sections of surface precipitation from GPROF2014 Version B2.

One known problem with the retrieval is shown in Figure 11 - where the Bayesian was unable to achieve a solution and produce a rain rate. The retrieval is from SSMIS, where there are 11 channels in the database which used to match the observed SSMIS Tbs. The only oceanic pixels in the SSMIS initial profile match were close to the USA coastline since they needed to be

matched with the NMQ radar observations. There were few of these matches in the Skin Temperature / TCWV bin where the retrieval is failing. The majority of the mid-latitude profiles in the database are from TMI where only the lower frequency channels are available. Therefore the observed Tbs for this orbit are trying to match the database Tbs from the TMI profiles with modeled 150, and 183 GHz channels. This channel modeling often shows that when the lower frequency channels (19,22,37) are matching well, the high frequency channels are off by 50 ^{o}K, thus the RMS difference of the observed Tb and the database Tbs is very large and no convergence on an answer if possible. Version B3 will address this and other problems.

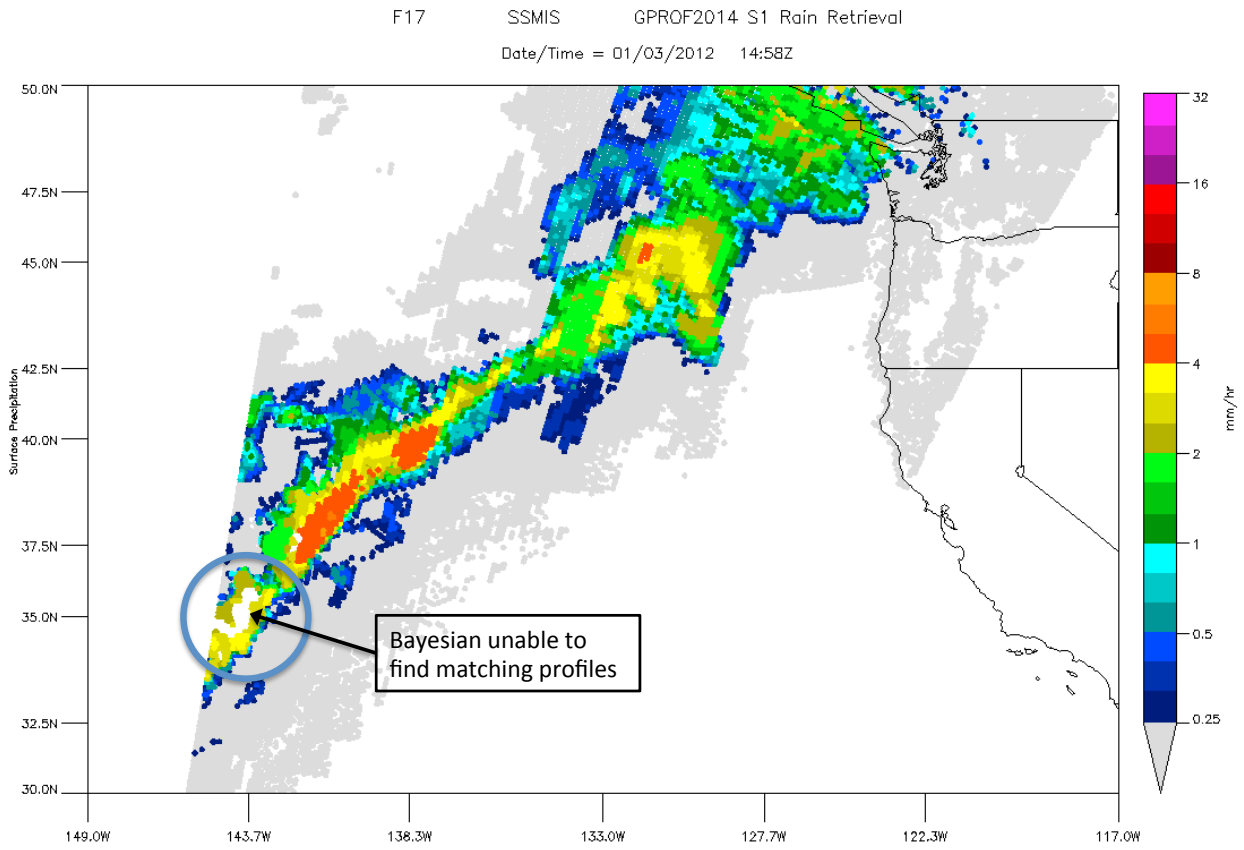

Figure 11. Pixels where the S1 retrieval was unable to produce a solution.

A few orbits of GMI simulated radiances were produced to test the GMI frequency Version B2 database. The retrieval successfully used these radiances to produce an orbit of rainrates (Figure 12).

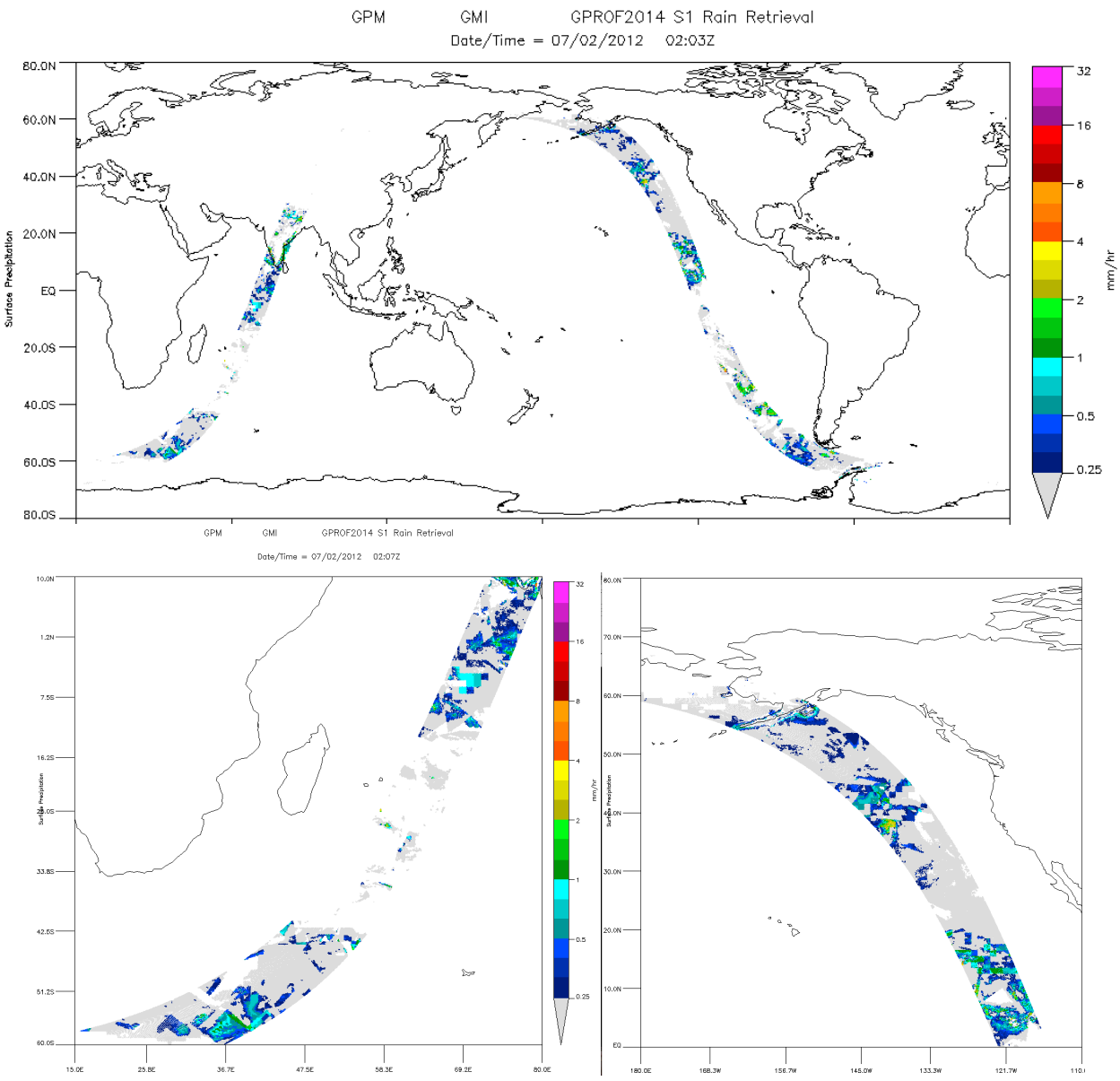

Figure 12. GPROF2014 Version B2 precipitation retrieval of simulated GMI radiances.

6.0 PLANNED ALGORITHM IMPROVEMENTS

6.1 Short-Term

The initial profile databases are quite large – up to 200,000 profiles in a given bin. For GPROF 2014 to run, one needs to cluster these entries to be efficient as was done in GPROF 2010. While clustering changes the final retrieval result only slightly, the step is cumbersome and not ideal for research purposes (*i.e.*, every time you try something new you have to go through a large clustering procedure before the algorithm can be run). Because of that, GPROF 2014 will have a research and an operational version. The research version works on a single surface temperature, TCWV, and Surface type. It runs successively over multiple bins but is rather slow – 30-60 minutes per orbit. The benefit is that the algorithm is easy to modify by all PIs for research purposes. The operational version will be created from the best research results and run only when needed for testing by the PPS. Version B2, which this document describes, is the science version of the algorithm.

The retrieval, as discussed at the GPM Algorithm Working Group Meeting in July 2011, has three variants to reflect that we either know nothing about the surface emissivity (S0), we know something about the surface emissivity (S1) or we have a Land Surface Model (LSM) to predict the key emissivity parameters (S2). Aside from using it in the retrieval, this LWM will have to be run for the period covering the databases. Specifically, the LSM variables would be added to all appropriate profiles in the same step as the other ancillary data is added to the hydrometeor profiles and T_b.

If we know nothing about the surface, we will run the algorithm variant (S0) that Grant Petty proposed that uses channels that effectively get rid of the surface variability. It looks at only the surface temperature and TCWV bin and combines all emissivity classes as these become irrelevant. By not dividing profiles into emissivity bins, the retrieval can be more robust and might be the first one to run as we build the databases in the GPM era.

Version B2, S0 Status: Channel reduction for the S0 retrieval is being completed by Grant Petty where Tb offsets calculated from the difference of the observed Tbs and the Model computed Tbs are used. Options for running the GPROF2014 retrieval in S0 or S1 are completed in the retrieval code.

If we know something about the emissivity (I take this to mean that we are in an emissivity class with good covariance between channels), the retrieval will look at the appropriate surface temperature, TCWV, and Surface Classification for a match. For Version B2, the emissivity classes are simply the mean emissivity cluster for that quarter degree grid. Co-variance of the emissivities are still pending for future versions.

The 15 surfaces classes were added to the CRM/MMF profiles (the model database), as well as the matching PI profiles. In this case, the retrieval itself would still search the appropriate surface temperature, TCWV, and Surface Class (emissivity) bin, and would use the similarity between databases and first guess emissivity as a weight in the Bayesian algorithm. This is still an S1 retrieval. If we really think we know the emissivity then it falls in the next class.

6.2 Longer-Term

Immediately after launch, an empirical database can be created using the DPR surface rain and hydrometeor profiles together with the observed GMI T_b. If the project is comfortable with using the existing Ku-band radar algorithm for Day 1, we can probably have enough profiles to start the GPM radiometer product V1 as soon as all the sensors are checked out. After the GPM launch, we will likely continue to use the model-based profiles, which will be enhanced through coincident overpasses between the GPM core satellite and available sounding radiometers. This will give us time until the "Combined" product is sufficiently mature to produce the physical databases needed to have confidence in the simulated T_b for the sounding radiometers.

Transition to later algorithms with the GPM database: For the first GPM-based *a-priori* database, the radiometer algorithm team will create an empirical database using DPR observed precipitation and GMI observations. Techniques that have been developed jointly with the X-cal team will be used to translate the observed GMI T_bs to equivalent T_b that would be observed by other constellation radiometers. This can be done quickly and will ensure that a good product is available from the radiometers soon after launch. Future versions will rely on physically constructed solutions from the "combined algorithm" team. Physical solutions not only ensure consistency between radar and radiometer, but also the retrieved geophysical parameters ensure that the computed T_b for the constellation radiometers is fully consistent with the *a-priori* database. Since the "combined algorithm" product becomes the *a-priori* database for GMI as well as the radiometer constellation, the radiometer algorithm should always be implemented six months after the reprocessing of the "combined algorithm." This represents a departure from the TRMM model where all algorithms are reprocessed simultaneously.

The transition to "fully physical" retrievals: The first database as described above is empirical in nature. By this we understand that a radiative transfer computation using the retrieved rainfall profiles from DPR do not necessarily yield the T_b observed by GMI. The reasons for the differences can be many, including; incorrect assumptions about drop size distributions, cloud water contents, ice microphysics, or surface properties. In some cases, such as tropical oceans, we have already developed techniques to adjust retrieved parameters so as to be simultaneously consistent with radar and radiometer observations on TRMM. These regions will be quickly transitioned (in the first reprocessing) from empirical to physical within GPM as well. The combined algorithm, however, will not always be able to create physically consistent solutions between DPR and GMI. An example is a complex coastline where emissivity is not known or calculable. The combined algorithm in this case will use only DPR to create a solution, leaving the *a-priori* database needed by the radiometer to be empirical. Because of this, the radiometer algorithm plans on a phased approach, starting with an empirically constructed *a-priori* database and transitioning this database to a physical one as we understand specific surfaces. The degree to which various surfaces are physically understood is shown below.

Emissivity models: Over oceans, good emissivity models exist that allow "combined retrievals" to produce physically consistent geophysical parameters. Over land, there are some surfaces where good knowledge exists (e.g. rain forests) while others (*e.g.*, semi-arid regions) still require

significant work before a truly physical model of the emissivity can be constructed. In the GPM combined algorithm, two steps are defined. The first step requires only covariances of the emissivities among channels. When these covariances are well defined and reduce the emissivity problem to one or two degrees of freedom, then physical databases can be constructed that retrieve these one or two degrees of freedom. This will be done first as different investigators provide guidance on the best way to define these degrees of freedom for individual surfaces. From an algorithm point of view, this is the only step that is required. From a GPM science point of view, we want to further know how the free parameters are related to geophysical parameters that can then be assimilated into Land Surface Models (LSMs). Conversely, if the relationship between emissivity and emissivity covariance and land surface parameters is known, then LSMs can be used to limit the degrees of freedom that have to be retrieved with respect to the surface in much the same way that a weather forecast model can already be used to specific atmospheric temperature structure. First, in order to use the useful covariances among channels and then the entire LSM, the retrieval algorithm must be able to identify the specific surfaces of applicability. We will track the portion of the globe that uses these physical methods versus the default empirical methods as part of the algorithm development.

6.3 Algorithm Version Delivery Timeline

Version B3: Scheduled update delivery to the PPS is June 30th, 2013. Documentation and software updates to the Science Team by July 31, 2013. Improvements for this delivery include:

a) Re-create the matched databases; fix known problems - Nai-Yu W., Mark K. Dave R.
b) Cross-Track Version of Preprocessor, GPROF2014 to the PPS – Chris K.
c) S0 improvements/implementation – SSMIS/TMI/AMSRE -> GMI - Grant P.
d) Implement Algorithm Precipitation Diagnostics
e) Create the set of new clustered hydrometeor profiles – Sarah R.
f) Apply new Hierarchical Clustering to Database Profiles – 2400 clusters per bin - Greg Elsaesser.

Version B4: Scheduled update delivery to the PPS by September 30th, 2013. Documentation and software updates available to the Science Team by October 15th*f*, 2013. Improvements for this delivery include:

a) Modify code for operational use and test– Dave R.
b) Interpolate Ancillary Model data in time. – Move to Model Prep Routine
c) Insert Orographic Lifting Index – Move to Model Prep Routine

7.0 REFERENCES

Aires, Filipe, Frédéric Bernardo, Héléne Brogniez, Catherine Prigent, 2010: An innovative calibration method for the inversion of satellite observations, *J. of Appl. Meteorol. and Climatology*, **49**, 2458-2473, doi: 10.1175/2010JAMC2435.1.

Aires, F., Prigent, C., Bernardo, F., Jiménez, C., Saunders, R. and Brunel, P., 2011: A tool to estimate land-surface emissivities at microwave frequencies (TELSEM) for use in numerical weather prediction. *Q. J. of the Roy. Meteorol. Soc.*, **137**: 690–699. doi: 10.1002/qj.803

Backus, G., and F. Gilbert, 1970: Uniqueness in the inversion of inaccurate gross earth data, *Philos. Trans. Roy. Soc. London*, A266, 123–192.

Berg, W., T. L'Ecuyer, and C. Kummerow, 2006. Rainfall climate regimes: The relationship of regional TRMM rainfall biases to the environment, *J. Appl. Meteor. Climatol.*, **45**, 434–454.

Boukabara, S.-A.; Fuzhong Weng; Quanhua Liu, 2007: Passive microwave remote sensing of extreme weather events using NOAA-18 AMSUA and MHS, *Geoscience and Remote Sensing, IEEE Transactions on* , **45**, 2228-2246, doi: 10.1109/TGRS.2007.898263.

Boukabara, S.-A.; Garrett, K.; Wanchun Chen; Iturbide-Sanchez, F.; Grassotti, C.; Kongoli, C.; Ruiyue Chen; Quanhua Liu; Banghua Yan; Fuzhong Weng; Ferraro, R.; Kleespies, T.J.; Huan Meng; 20011: MiRS: an all-weather 1DVAR satellite data assimilation and retrieval system, *Geoscience and Remote Sensing, IEEE Transactions on* , **49**, 3249-3272, doi:10.1109/TGRS.2011.2158438

Hiley, M. J., M. S. Kulie, and R. Bennartz, 2011: Uncertainty Analysis for CloudSat Snowfall Retrievals. *J Appl Meteorol Clim*, **50,** 399-418.

Hollinger, J.P. 1989: *DMSP Special Sensor Microwave/Imager Calibration/Validation*. Final Report, Vol. I., Space Sensing Branch, Naval Research Laboratory, Washington D.C.

Kummerow, C., W.S. Olson and L. Giglio, 1996. A simplified scheme for obtaining precipitation and vertical hydrometeor profiles from passive microwave sensors, *IEEE, Trans on Geoscience and Remote Sensing,* **34**, 1213-1232, doi: 10.1109/36.536538.

Kummerow, C., W. Barnes, T. Kozu, J. Shiue and J. Simpson, 1998. The tropical rainfall measuring mission (TRMM) sensor package, *J. Atmos. Oceanic Technol.*, **15**, 809–817.

L'Ecuyer, T. S., G. L. Stephens, 2002: An estimation-based precipitation retrieval algorithm for attenuating radars. *J.Appl.Meteorol.,* **41**, 272-285.

Lorenc, A. C., 1986: Analysis methods for numerical weather prediction. *Quart. J. Roy. Meteor. Soc.*, **112**, 1177-1194.

Prigent, C., C., W. B. Rossow, and E. Matthews, 1997: Microwave land surface emissivities estimated from SSM/I observations. *J. Geophys. Res.*, **102**, 21 867 – 21 890.

Prigent, C., E. Jaumouille, F. Chevallier, and F. Aires, 2008: A parameterization of the microwave land surface emissivity between 19 and 100 GHz, anchored to satellite-derived estimates*, IEEE Transaction on Geoscience and Remote Sensing* , **46**, 344-352, doi:10.1109/TGRS.2007.908881.

Rapp, A., M. Lebsock, C. Kummerow, 2009: On the Consequences of Resampling Microwave Radiometer Observations for Use in Retrieval Algorithms, *J. of Appl. Meteo. and Clim.,* **48**, 2242-2256, doi: 10.1175/2009JAMC2156.1.

Reynolds, R.W., T.M. Smith, C. Liu, D.B. Chelton, K.S. Casey, and M.G. Schlax, 2006: Daily high-resolution-blended analyses for sea surface temperature. *J. Climate,* **20,** 5473- 5496.

Sudradjat, Arief, Nai-Yu Wang, Kaushik Gopalan, Ralph R. Ferraro, 2011: Prototyping a generic, unified land surface classification and screening methodology for GPM-era microwave land precipitation retrieval algorithms, *J. Appl. Meteorol. and Climatology*, **50**, 1200-1211, doi: 10.1175/2010JAMC2572.1

Weng, F., B. Yan, and N.C. Grody, 2001: A microwave land emissivity model. *J. Geophys. Res.*, **106**, 20 115 – 20 123.

APPENDIX A : CONSTELLATION RADIOMETER DESCRIPTIONS

A.1 GPM Microwave Imager

The GPM Microwave Imager (GMI) instrument is a multi-channel, conical-scanning, microwave radiometer serving an essential role in the near-global-coverage and frequent-revisit-time requirements of GPM (Fig. A.1). The instrumentation enables the Core spacecraft to serve as both a 'precipitation standard' and as a 'radiometric standard' for the other GPM constellation members. The GMI is characterized by thirteen microwave channels ranging in frequency from

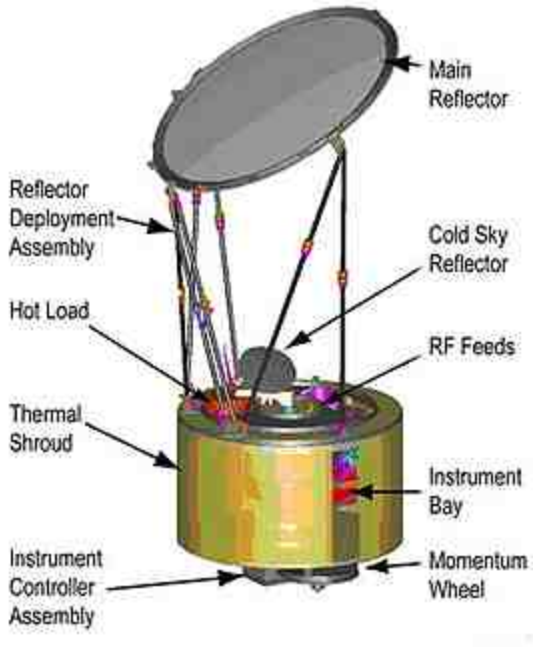

Fig. A.1 GMI instrument.

Table A.1. GMI performance characteristics.

Frequency (GHz)	Polarization	NEDT/ Reqmt (K)	Expected* NEDT	Expected Beam Efficiency (%)	Expected Calibration Uncert.	Resolution (km)
10.65	V/H	0.96	0.96	91.4	1.04	26
18.7	V/H	0.84	0.82	92.0	1.08	15
23.8	V	1.05	0.82	92.5	1.26	12
36.5	V/H	0.65	0.56	96.6	1.20	11
89.0	V/H	0.57	0.40	95.6	1.19	6
165.5	V/H	1.5	0.81	91.9	1.20	6
183.31±3	V	1.5	0.87	91.7	1.20	6
183.31±7	V	1.5	0.81	91.7	1.20	6

10 GHz to 183 GHz (see Table A.1). In addition to carrying channels similar to those on the Tropical Rainfall Measuring Mission (TRMM) Microwave Imager (TMI), the GMI carries four

high frequency, millimeter-wave channels at about 166 GHz and 183 GHz. With a 1.2 m diameter antenna, the GMI will provide significantly improved spatial resolution over TMI. Launch date for the core spacecraft: February, 2014.

A.2 The Advanced Microwave Scanning Radiometer 2

The Advanced Microwave Scanning Radiometer 2 (AMSR 2), which will flies on the GCOM-W1 platform is a sensor to observe microwave radiation at six different frequency bands ranging from 7 GHz to 89 GHz. AMSR 2 is designed to monitor Earth's hydrological cycle including sea surface temperature, cloud water, water vapor, precipitation, sea-ice, and soil moisture.

The antenna of the AMSR 2, which receives microwave radiation from the ground, arc scans the ground surface at a ratio of one turn every 1.5 seconds and observes an area approximately 1,450 kilometers wide in one scan. Using this scanning method, the AMSR 2 can observe over 99% of the Earth's area in just two days. The diameter of the antenna is about 2 m, making it the world's largest observation sensor aboard a satellite. The height of the rotating part is about 2.7 m and the weight is about 250 kg. The AMSR 2 can keep rotating such a large and heavy antenna at a speed of one turn per 1.5 s for 24 hours a day and more than five years without a minute of rest.

Table A.1. AMSR 2 performance characteristics

Orbit	Launch	Design life (yrs)	Local time (LTAN)	Swath width (km)	Antenna	Incidence angle (deg)
Sun Synchronous with 699.6km altitude (over equator)	JFY201	5	13:30	1450	2.0m offset parabola	Nominal 55

Table A.2. AMSR 2 Channel Set

Center Freq. (GHz)	Bandwidth (MHz)	Polarization	Beam Width (deg.) (ground res. [km])	Sampling Interval (km)
6.925/7.3	350	V/H	1.8 (35 x 62)	10
6.925/7.3	350	V/H	1.7 (34 x 58)	10
10.65	100	V/H	1.2 (24 x 42)	10
18.7	200	V/H	0.65 (14 x 22)	10
23.8	400	V/H	0.75 (15 x 26)	10
36.5	1000	V/H	0.35 (7 x 12)	10

89.0	3000	V/H	0.15 (3 x 5)	5

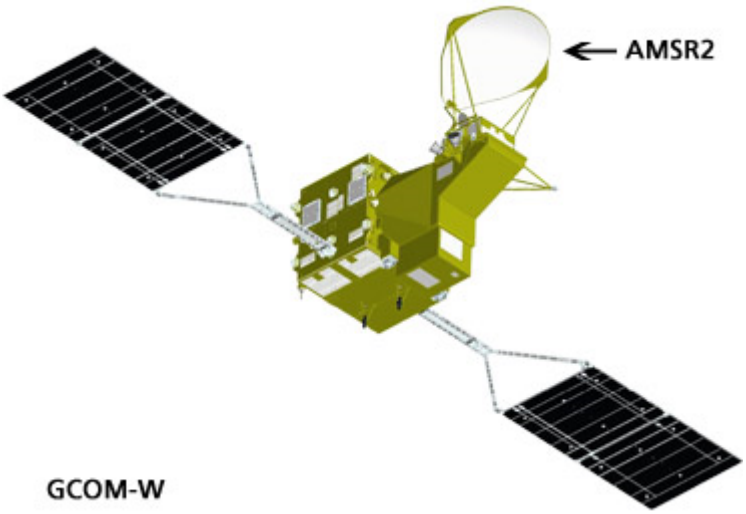

Fig. A.1. AMSR 2

A.3 MADRAS

MADRAS is a microwave imager, with conical scanning (incidence angle 56°), close to the SSM/I and TMI concepts. The main aim of the mission is the study of cloud systems. A frequency has been added (157 GHz) in order to study the high-level ice clouds associated with deep convective systems, and to serve as a window channel relative to the sounding instrument at 183 GHz.

Table A.3. Main characteristics of the MADRAS channels

Frequencies	Polarization	Pixel size (km)	Main use
18.7 GHz ± 100 MHz	H/V	40	ocean rain and surface wind
23.8 GHz ± 200 MHz	V	40	integrated water vapor
36.5 GHz ± 500 MHz	H/V	40	cloud liquid water
89 GHz ± 1350 MHz	H/V	10	convective rain areas
157 GHz ± 1350 MHz	H/V	6	cloud top ice

The main uses given here are only descriptive. In practice most of the products will be extracted from algorithms combining the different channels information. The resolutions are those expected in the different channels, accounting for the specification of 10 km given for the 89-GHz channel.

The general Geometry of scanning of the three instruments of the mission is represented in Fig. A.2.

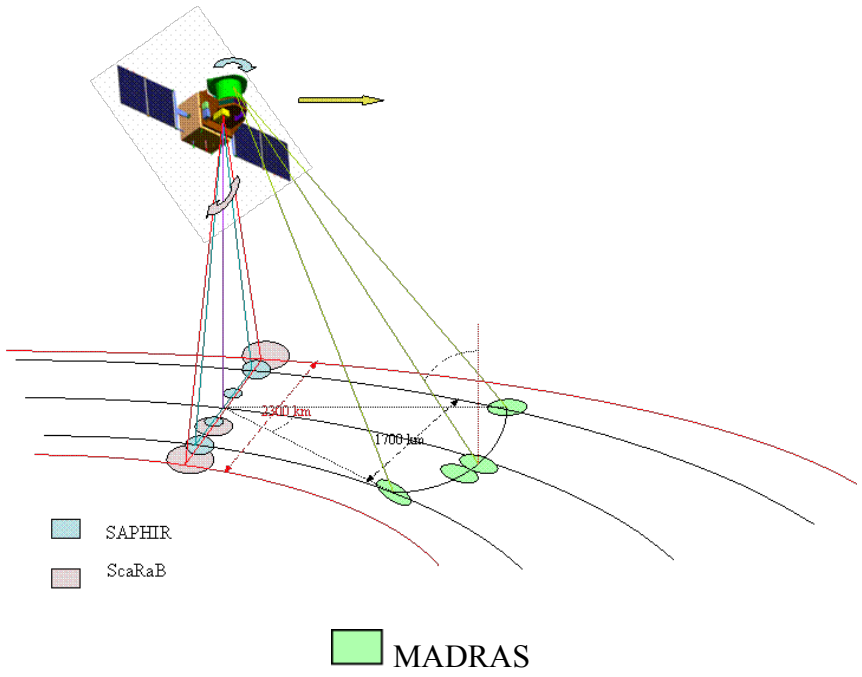

Fig. A.2. General configuration of the swath of the three instruments of Megha-Tropiques. Size of the footprints has been enhanced in order to show their geometric behavior.

Spectral characteristics include three instruments that compose the core payload of the mission: a microwave imager, a microwave water vapor sounder, a radiative budget radiometer. Preliminary studies have defined the main characteristics of these instruments. Launch date: Scheduled for the second half of 2010.

A.4 Sondeur Atmosphérique Du Profil D'humidité Intertropicale Par Radiométrie (SAPHIR)

Sondeur Atmosphérique du Profil d'Humidité Intertropicale par Radiométrie (SAPHIR) is a sounding instrument with six channels near the absorption band of water vapor at 183 GHz. These channels provide relatively narrow weighting functions from the surface to about 10 km, allowing retrieving water vapor profiles in the cloud free troposphere. The scanning is cross-track, up to an incidence angle of 50°. The resolution at nadir is of 10 km.

The atmospheric opacity spectrum (see Fig. A.3) shows a first water vapor absorption line centered at 22.235 GHz, and a second one at 183.31 GHz (pure rotation line). Between these two lines, the water vapor continuum slowly increases absorption by the atmosphere with frequency. The first water vapor line is too low to permit profiling, and its partial transparency is used to obtain the total columnar content. The second line is high enough to enable sounding in the first 10-12 km of the atmosphere. The sounding principle consists of selecting channels at

different frequencies inside the absorption line, in order to obtain a maximal sensitivity to humidity at different heights. Previous microwave sounders are SSMT2 and AMSU-B, which are operational instruments and have three channels within the 183.31 GHz absorption line (at ±1, ±3 and ±7 GHz), and two window channels, at 150 and 89 GHz. These additional channels give information on the surface and near surface.

Table A.4. Channel selection for SAPHIR on board Megha/Tropiques.

Channel	Center Freq. (GHz)	Bandwidth (MHz)	Sensitivity (K)	Polarization
S1	183.31±0.2	200	1.82	H
S2	183.31±1.1	350	1.01	H
S3	183.31±2.7	500	0.93	H
S4	183.31±4.0	700	0.88	H
S5	183.31±6.6	1200	0.81	H
S6	183.31±11.0	2000	0.73	H

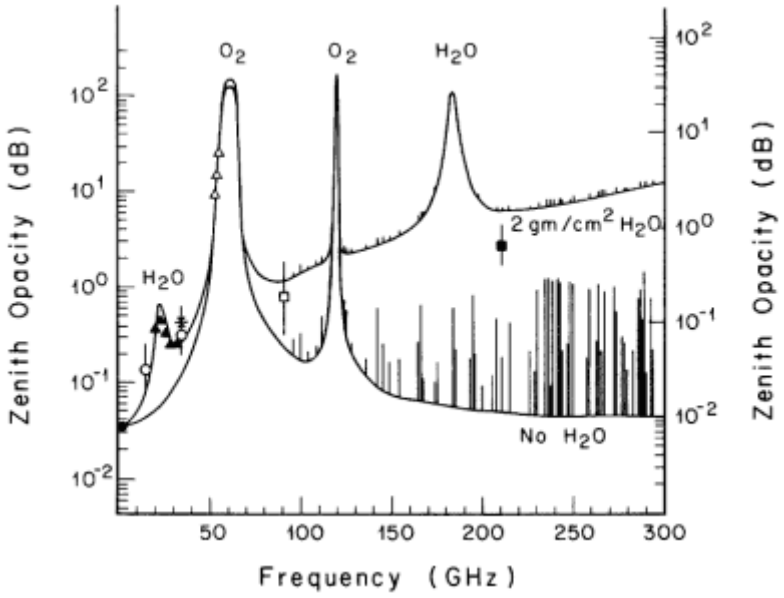

Fig. A.3. The atmospheric opacity for a US standard atmosphere.

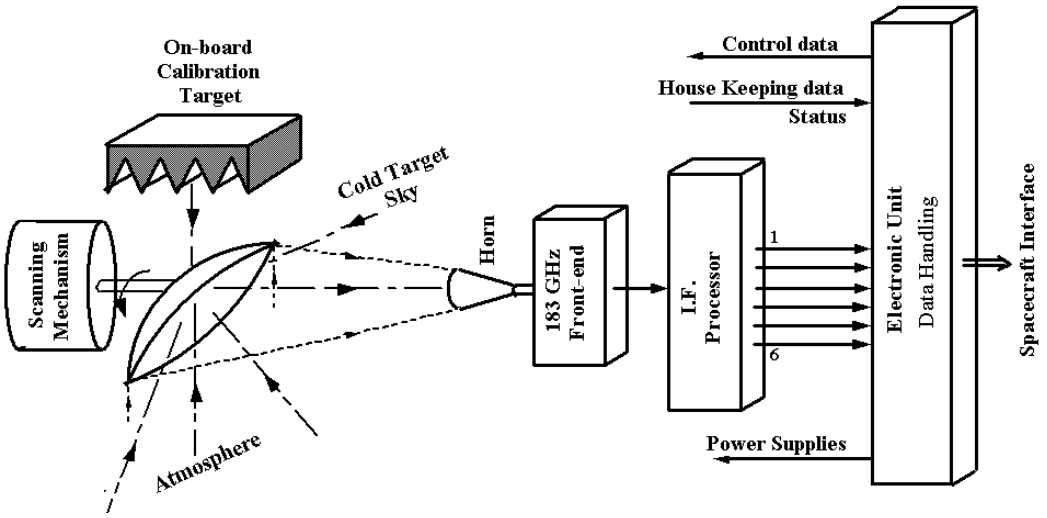

Fig. A.4. SAPHIR instrument.

A.5 Special Sensor Microwave Imager/Sounder

The Special Sensor Microwave Imager/Sounder (SSMIS) is a conically scanning passive microwave radiometer with a 53.1° earth incidence angle sensing upwelling microwave radiation at 24 channels covering a wide range of frequencies from 19-183 GHz. The Level 1C dataset contains only 11 of these channels, which are most relevant to sensing precipitation. Data is collected along an active scan of 144 degrees across track producing a swath width on the ground of 1707 km. The first of five sensors were launched on board DMSP F16 on October 18, 2003. The SSMIS is a joint US Air Force/Navy multi-channel passive microwave sensor that combines and extends the imaging and sounding capabilities of three separate DMSP microwave sensors including the SSM/T, SSM/T2, and SSM/I. It was built by Northrup-Grumman Electronic Systems.

Table A.5. SSMIS characteristics from the Algorithm and Data User Manual for SSMIS (2002). (Note: The channels in the Level 1C dataset are a subset of the full SSMIS channel complement.)

Center Freq. (GHz)	Polarization	Bandwidth (MHz)	IFOV (km x km)	EFOV* (km x km)	Sensitivity (K)
19.35	V/H	350	73x47	45x74	0.35
22.235	V	410	73x47	45x74	0.45
37.0	V/H	160	41x31	28x45	0.22
91.665	V/H	1410	14x13	13x16	0.19
150	H	1640	14x13	13x16	0.53
183.311 ± 1	H	510	14x13	13x16	0.38
183.311 ± 3	H	1020	14x13	13x16	0.39
183.311 ± 7	H	1530	14x13	13x16	0.56

*EFOV values are km along scan x km across scan.

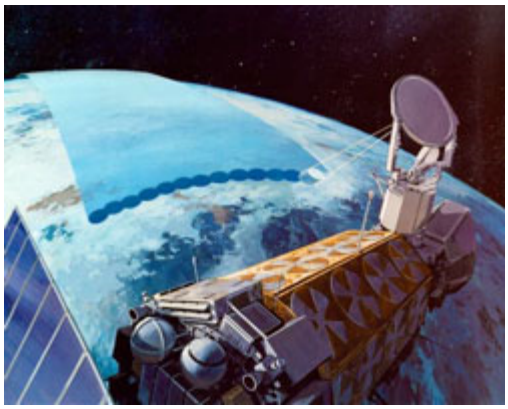

Fig. A.5. SSMIS.

A.6 WindSat

WindSat is a multi-frequency polarimetric microwave radiometer designed to demonstrate the capability of polarimetric microwave radiometry to measure the ocean surface wind vector from space. It has 22 channels operating at five frequencies. All frequencies have both V and H polarizations and three of the channels also have ±45, left-hand circular and right-hand circular polarizations. The instrument scans both before and after, and while some frequency bands have a swath width greater that 1200 km, the common swath width is approximately 950 km (68° of scan angle) and the aft common swath is 350 km (23° of scan angle). It was launched on board the U.S. Department of Defense Coriolis satellite on January 6, 2003 into an 840 km circular sun-synchronous orbit.

Table A.6. WindSat performance characteristics.

Center Freq. (GHz)	Polarization	Bandwidth (MHz)	Sensitivity (K)	IFOV (km x km)	Earth Incidence Angle (deg)
6.8	V/H	125	0.48	60x40	53.5
10.7	V/H/±45/L/R	300	0.37	38x25	49.9
18.7	V/H/±45/L/R	750	0.39	27x16	55.3
23.8	V/H	500	0.55	20x12	53.0
37.0	V/H/±45/L/R	2000	0.45	13x8	53.0

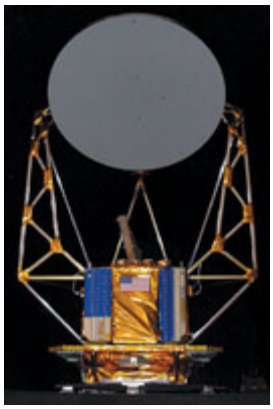

Fig. A.6. WindSat.

A.7 Advanced Microwave Scanning Radiometer-EOS

The Advanced Microwave Scanning Radiometer-E (AMSR-E) was a conically scanning total power passive microwave radiometer sensing microwave radiation (brightness temperatures) at 12 channels and 6 frequencies ranging from 6.9 to 89.0 GHz. Horizontally and vertically polarized radiation are measured separately at each frequency. There are two separate horns at 89 GHz, one being slightly offset from the centerline of the feedhorn array. *(As of 25 October 2004, there are no data from the 89-GHz horn A. The science algorithms have been modified to take this into account).*

The AMSR-E instrument (Fig. A.7) modified from the design used for the ADEOS-II AMSR, has an offset parabolic reflector 1.6 meters in diameter. Figure A.8 shows the Aqua satellite with AMSR-E mounted in front. The atmospheric radiation is focused by the main reflector into an array of six feedhorns (Fig. A.9), which then feed the radiation to the detectors.

Fig. A.7. AMSR-E Instrument.

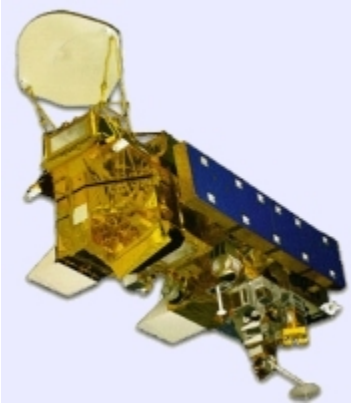

Fig. A.8. AMSR-E on the Aqua Satellite.

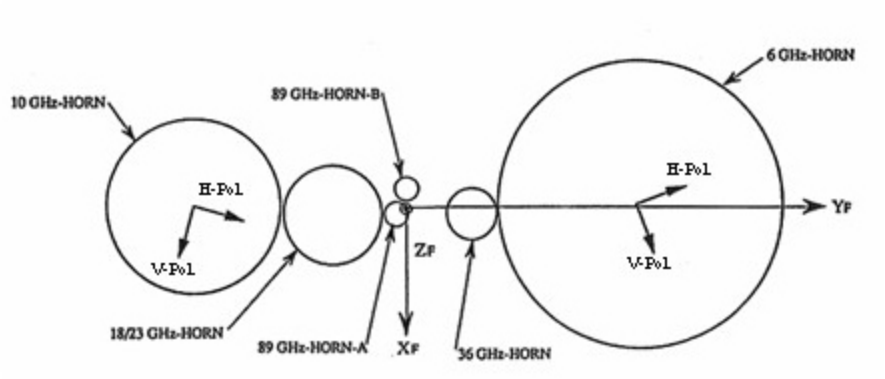

Fig. A.9. AMSR-E Horn Configuration.

A cold load reflector and a warm load are mounted on the transfer assembly shaft and do not rotate with the drum assembly. They are positioned off axis such that they pass between the feedhorn array and the parabolic reflector, occulting it once each scan. The cold load reflector reflects cold sky radiation into the feedhorn array thus serving, along with the warm load, as calibration references for the AMSR-E. Calibration of the radiometers is essential for collection of useful data. Corrections for spillover and antenna pattern effects are incorporated in the data processing algorithms.

The AMSR-E rotates continuously about an axis parallel to the local spacecraft vertical at 40 revolutions per minute (rpm). At an altitude of 705 km, it measures the upwelling scene

brightness temperatures over an angular sector of ±61 degrees about the sub-satellite track, resulting in a swath width of 1445 km.

During a period of 1.5 seconds the spacecraft sub-satellite point travels 10 km. Even though the instantaneous field-of-view for each channel is different, active scene measurements are recorded at equal intervals of 10 km (5 km for the 89-GHz channels) along the scan. The half cone angle at which the reflector is fixed is 47.4°, which results in an Earth incidence angle of 55.0°. Launch date: May 4, 2002. Table A.7 lists the pertinent performance characteristics.

Table A.7. AMSR-E performance characteristics.

Center Freq. (GHz)	Bandwidth (MHz)	Sensitivity (K)	Mean Spatial Resol-ution (km)	IFOV (km x km)	Sampling Rate (km x km)	Integration Time (m/sec)	Main Beam Efficiency (%)	Beam Width (deg.)
6.925	350	0.3	56	74 x 43	10 x 10	2.6	95.3	2.2
10.65	100	0.6	38	51 x 30	10 x 10	2.6	95.0	1.4
18.7	200	0.6	21	27 x 16	10 x 10	2.6	96.3	0.8
23.8	400	0.6	24	31 x 18	10 x 10	2.6	96.4	0.9
36.5	1000	0.6	12	14 x 8	10 x 10	2.6	95.3	0.4
89.0	3000	1.1	5.4	6 x 4	5 x 5	1.3	96.0	0.18

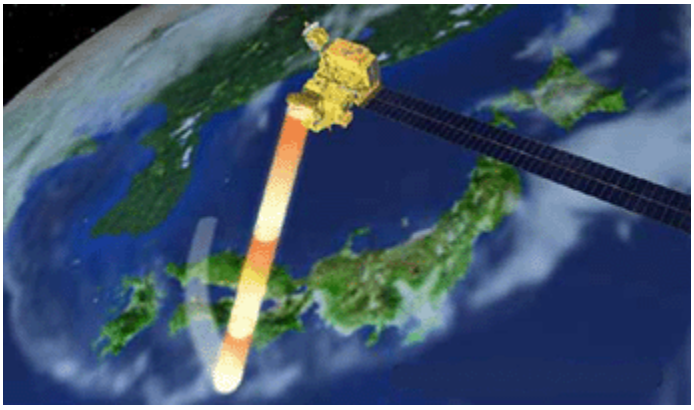

Fig. A.10. AMSR-E.

A.8 Advanced Microwave Sounding Unit

The Advanced Microwave Sounding Unit (AMSU) is a multi-channel microwave radiometer installed on meteorological satellites. The instrument examines several bands of microwave radiation from the atmosphere to perform atmospheric sounding of temperature and moisture levels. AMSU data is used extensively in weather prediction. Brightness temperatures are processed as quickly as possible and sent to numerical weather prediction (NWP) centers around the world. This data helps keep the assessment of the current state of the atmosphere correct,

which in turn helps make predictions more accurate. Long-term AMSU records are also used in studies of climate.

The AMSU has two sub-instruments, AMSU-A and AMSU-B. AMSU-A has 15 channels between 23.8 and 89 GHz, and is used primarily for measuring atmospheric temperatures (known as "temperature sounding"). It has a ground resolution near nadir of 45 km. AMSU-B, with five channels between 89 and 183.3 GHz, has a spatial resolution near nadir of 15 km and is primarily intended for moisture sounding. Spot size of both sub-instruments becomes larger and more elongated toward the edges of the swath. When the two instruments are used together, there are roughly nine AMSU-B fields-of-view in a 3x3 array corresponding to each AMSU-A field-of-view. This reflects the higher spatial variability of water vapor compared to temperature. HIRS/3 infrared sounders with the same spatial resolution as AMSU-B are also included on NOAA 15-17 satellites and are used together with AMSU-A and AMSU-B. Together the three instruments form ATOVS, the Advanced TIROS Operational Vertical Sounder.

The Aqua and MetOp AMSU-A instruments are 15-channel microwave sounders designed primarily to obtain temperature profiles in the upper atmosphere (especially the stratosphere) and to provide a cloud-filtering capability for tropospheric temperature observations. The EOS AMSU-A is part of a closely coupled triplet of instruments that include the AIRS and HSB. The MetOp AMSU-A similarly works with HIRS, IASI, and MHS. MHS and HSB are variants on AMSU-B.

Table A.8. Radiometric characteristics of the AMSU-A.

Channel	Freq. (GHz)	Polarization (at nadir)	Band #	Sensitivity (K)	Primary Function
1	23.8	V	1	0.30	Water vapor burden
2	31.4	V	1	0.30	Water vapor burden
3	50.3	V	1	0.40	Water vapor burden
4	52.8	V	1	0.25	Water vapor burden
5	53.596 ± 0.115	H	2	0.25	Tropospheric Temperature
6	54.4	H	1	0.25	Tropospheric Temperature
7	54.94	V	1	0.25	Tropospheric Temperature
8	55.5	H	1	0.25	Tropospheric Temperature
9	57.290	H	1	0.25	Stratospheric Temperature
10	57.290 ± 0.217	H	2	0.40	Stratospheric Temperature
11	57.290 ± 0.3222 ± 0.048	H	4	0.40	Stratospheric Temperature
12	57.290 ± 0.3222 ± 0.022	H	4	0.60	Stratospheric Temperature
13	57.290 ± 0.3222 ± 0.010	H	4	0.80	Stratospheric Temperature
14	57.290 ± 0.3222 ± 0.0045	H	4	1.20	Stratospheric Temperature
15	89.0	V	1	0.60	Cloud top/snow

Table A.9. Radiometric characteristics of the AMSU-B.

Channel	Freq. (GHz)	Polarization (at nadir)	Band #	Sensitivity (K)
16	89.9 ± 0.9	V	2	0.37
17	150 ± 0.9	V	2	0.84
18	183.31 ± 1.00	V	2	1.06
19	183.31 ± 3.00	V	2	0.70
20	183.31 ± 7.00	V	2	0.60

A.9 TRMM Microwave Imager

The TRMM Microwave Imager (TMI) is a nine-channel passive microwave radiometer based upon the Special Sensor Microwave/Imager (SSM/I), which has been flying aboard the U.S. Defense Meteorological Satellite Program (DMSP) satellites since 1987. The key differences are the addition of a pair of 10.7-GHz channels with horizontal and vertical polarizations and a frequency change of the water vapor channel from 22.235 to 21.3 GHz. This change off the center of the water vapor line was made in order to avoid saturation in the tropical orbit of TRMM. Table A.10 presents the performance characteristics of the nine TMI channels. The increased spatial resolution evident in Table A.10 is due to the lower orbit of the TRMM satellite with respect to the DMSP rather than sensor differences.

The TMI antenna (Fig. A.11) is an offset parabola, with an aperture size of 61 cm (projected along the propagation direction) and a focal length of 50.8 cm. The antenna beam views the earth's surface with a nadir angle of 498, which results in an incident angle of 52.88 at the earth's surface. The TMI antenna rotates about a nadir axis at a constant speed of 31.6 rpm. The rotation draws a circle on the earth's surface. Only 1308 of the forward sector of the complete circle is used for taking data. The rest is used for calibrations and other instrument housekeeping purposes. From the TRMM orbit, the 130 scanned sector yields a swath width of 758.5 km shown in Fig. A.12. During each complete revolution (*i.e.*, a scan period of about 1.9 s), the sub-satellite point advances a distance *d* of 13.9 km. Since the smallest footprint (85.5-GHz channels) size is only 6.9 km (down-track direction) by 4.6 km (cross-track direction), there is a gap of 7.0 km between successive scans. However, this is the only frequency where there is a small gap. For all higher-frequency channels, footprints from successive scans overlap the previous scans. Launch date: 1997, active.

Table A.10. TMI performance characteristics.

Channel	Center Freq. (GHz)	Polari-zation	Bandwidth (MHz)	Sensitivity (K)	IFOV (km x km)	Sampling Interval (km x km)	Integr-ation Time (m/sec)	Main Beam Effic-iency (%)	Beam width (deg)
1	10.65	V	100	0.63	63 x 37	13.9x9.1	6.6	93	3.68
2	10.65	H	100	0.54	63 x 37	13.9x9.1	6.6	93	3.75
3	19.35	V	500	0.50	30 x 18	13.9x9.1	6.6	96	1.90
4	19.35	H	500	0.47	30 x 18	13.9x9.1	6.6	96	1.88
5	21.3	V	200	0.71	23 x 18	13.9x9.1	6.6	98	1.70
6	37.0	V	2000	0.36	16 x 9	13.9x9.1	6.6	91	1.00
7	37.0	H	2000	0.31	16 x 9	13.9x9.1	6.6	92	1.00
8	85.5	V	3000	0.52	7 x 5	13.9x4.6	3.3	82	0.42
9	85.5	H	3000	0.93	7 x 5	13.9x4.6	3.3	85	0.43

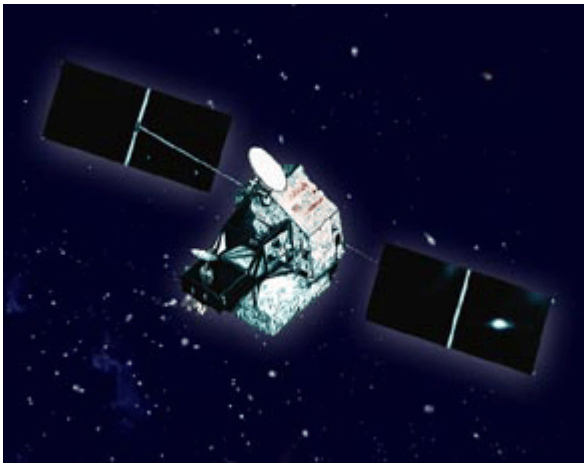

Fig. A.11. TMI.

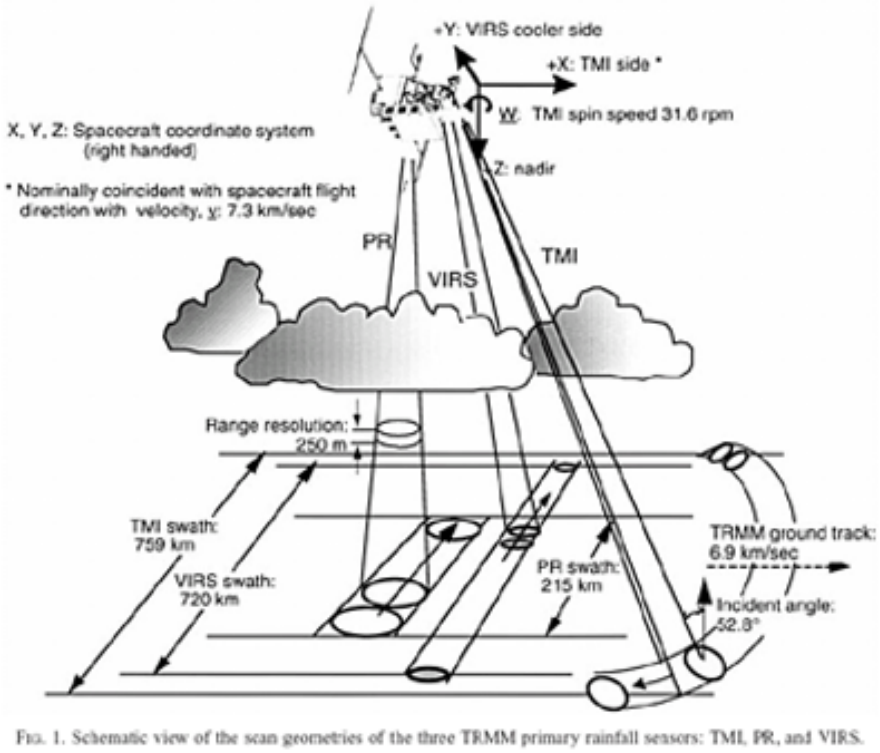

FIG. 1. Schematic view of the scan geometries of the three TRMM primary rainfall sensors: TMI, PR, and VIRS.

Fig. A.12. Schematic view of the scan geometries of the three TRMM primary rainfall sensors: TMI, PR, and VIRS. Figure provided by Kummerow *et al.* (1998).

A.10 Special Sensor Microwave/Imager

The Special Sensor Microwave/Imager (SSM/I) is a seven-channel, four-frequency, linearly polarized passive microwave radiometric system. The instrument measures surface/atmospheric

microwave T_bs at 19.35, 22.235, 37.0 and 85.5 GHz. The four frequencies are sampled in both horizontal and vertical polarizations, except the 22 GHz, which is sampled in the vertical only.

The SSM/I has been a very successful instrument, superseding the along cross-track and Dicke radiometer designs of previous systems. Its combination of constant-angle rotary-scanning and total power radiometer design has become standard for passive microwave imagers, (*e.g.,* TRMM Microwave Imager, AMSR). Information within the SSM/I T_bs measurements allow the retrieval of four important meteorological parameters over the ocean: near-surface wind speed (note scalar not vector), total columnar water vapor, total columnar cloud liquid water (liquid water path) and precipitation. However, accurate and quantitative measurement of these parameters from the SSM/I T_bs is a non-trivial task. Variations within the meteorological parameters significantly modify the T_bs. As well as open ocean retrievals, it is also possible to retrieve quantitatively reliable information on sea ice, land snow cover and over-land precipitation.

The instrument is flown onboard the United States Air Force Defense Meteorological Satellite Program (DMSP) Block 5D-2 spacecraft. These are in circular or near-circular Sun-synchronous and near-polar orbits at altitudes of 833 km with inclinations of 98.8° and orbital periods of 102.0 minutes, each making 14.1 full orbits per day. The scan direction is from the left to the right with the active scene measurements lying ±51.2 degrees about when looking in the F8 forward (F10-F15) or aft (F8) direction of the spacecraft travel. This results in a nominal swath width of 1394 km allowing frequent ground coverage, especially at higher latitudes. All parts of the globe at latitudes greater than 58° are covered at least twice daily except for small unmeasured circular sectors of 2.4° about the poles. Extreme polar regions (> 72° N or S) receive coverage from two or more overpasses from both the ascending and descending orbits each day.

The spin rate of the SSM/I provides a period of 1.9 s during which the DMSP spacecraft sub-satellite point travels 12.5 km. Each scan 128 discrete, uniformly spaced radiometric samples are taken at the two 85-GHz channels and, on alternate scans, 64-discrete samples are taken at the remaining five lower frequency channels. The resolution is determined by the Nyquist limit and the Earth's surface contribution of 3-dB bandwidth of the signal at a given frequency (see Table A.11). The radiometer direction intersects the Earth's surface at a nominal incidence angle of 53.1 degrees, as measured from the local Earth normal.

Table A.11. Radiometric performance characteristics of the SSM/I (Hollinger 1989).

Center Freq. (GHz)	**Polarization**	**IFOV (km x km)**	**Spatial Sampling (km)**	**Sensitivity (K)**
19.35	H	69x43	25	0.42
19.35	V	69x43	25	0.45
22.235	V	50x40	25	0.74
37.0	H	37x28	25	0.38
37.0	V	37x28	25	0.37
85.5	H	15x13	12.5	0.73
85.5	V	15x13	12.5	0.69

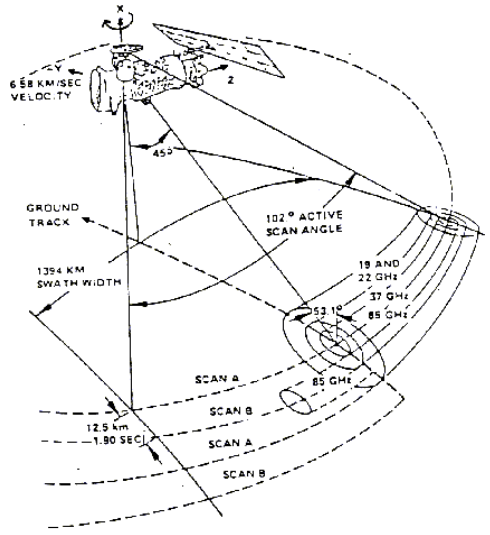

Fig. A13. The scan geometry of the SSM/I.

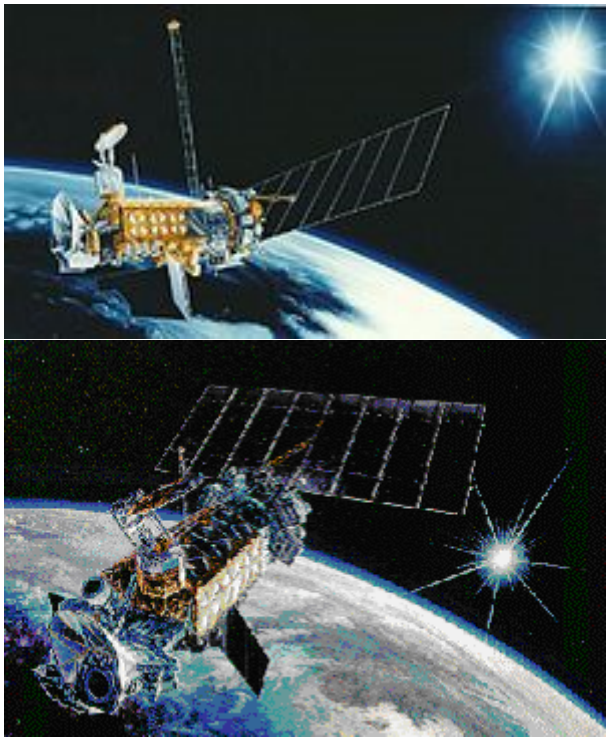

Fig. A.14. SSM/I.

A.11 Advanced Technology Microwave Sounder

The Advanced Technology Microwave Sounder (ATMS) will operate in conjunction with the Cross-track Infrared Sounder (CrIS) to profile atmospheric temperature and moisture. The ATMS is the next generation cross-track microwave sounder that will combine the capabilities of current generation microwave temperature sounders (Advanced Microwave Sounding Unit – AMSU-A) and microwave humidity sounders (AMSU-B) that are flying on NOAA's Polar Operational Environmental Satellites (POES). The ATMS draws its heritage directly from AMSU-A/B, but with reduced volume, mass and power. The ATMS has 22 microwave channels to provide temperature and moisture sounding capabilities. Sounding data from CrIS and ATMS will be combined to construct atmospheric temperature profiles at 1 K accuracy for 1 km layers in the troposphere and moisture profiles accurate to 15% for 2 km layers. Higher (spatial, temporal and spectral) resolution and more accurate sounding data from CrIS and ATMS will support continuing advances in data assimilation systems and Numerical Weather Prediction (NWP) models to improve short- to medium-range weather forecasts.

Both CrIS and ATMS (CrIMSS) are selected to fly on the National Polar-orbiting Operational Environmental Satellite System (NPOESS) spacecraft, combining both cross-track infrared and microwave sensors aboard the NPOESS satellite. Expected NPP launch year is 2011.

Table A.12. Instrument characteristics of the ATMS.

Channel	Center Freq. (GHz)	Bandwidth (GHz)	Center Freq. Stability (MHz)	Temp. Sensitivity (K)
1	23.8	0.27	<10	0.7
2	31.4	0.18	<10	0.8
3	50.3	0.18	<10	0.9
4	51.76	0.4	<5	0.7
5	52.8	0.4	<5	0.7
6	53.596±0.115	0.17	<5	0.7
7	54.4	0.4	<5	0.7
8	54.94	0.4	<10	0.7
9	55.5	0.33	<10	0.7
10	57.290344	0.33	<0.5	0.75
11	57.290344±0.217	0.078	<0.5	1.2
12	57.290344±0.3222±0.048	0.036	<1.2	1.2
13	57.290344±0.03222±0.022	0.016	<1.6	1.5
14	57.290344±0.03222±0.010	0.008	<0.5	2.4
15	57.290344±0.03222±0.0045	0.003	<0.5	3.6
16	88.2	2.0	<200	0.5
17	165.5	3.0	<200	0.6
18	183.31±7	2.0	<30	0.8
19	183.31±4.5	2.0	<30	0.8
20	183.31±3	1.0	<30	0.8
21	183.31±1.8	1.0	<30	0.8
22	183.31±1	0.5	<30	0.9

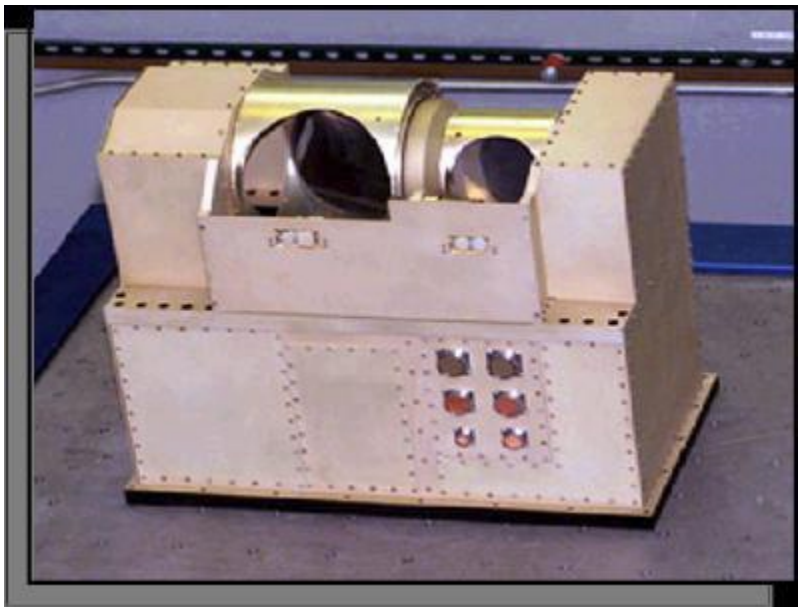

Fig. A.15. ATMS Instrument.

A.12 Microwave Humidity Sounder

MHS - The Microwave Humidity Sounder (MHS) is one of the European instruments carried on MetOp-A. MHS is a five-channel, total power, microwave radiometer designed to scan through the atmosphere to measure the apparent upwelling microwave radiation from the Earth at specific frequency bands. Since humidity in the atmosphere (ice, cloud cover, rain and snow) attenuate microwave radiation emitted from the surface of the Earth, it is possible, from the observations made by MHS, to derive a detailed picture of atmospheric humidity with the different channels relating to different altitudes. Temperature at the surface of the Earth can also be determined.

MHS works in conjunction with four of the U.S. instruments provided by the National Oceanic and Atmospheric Administration (NOAA), namely the Advanced Microwave Sounding Unit–A1 (AMSU-A1), the Advanced Microwave Sounding Unit–A2 (AMSU-A2), the Advanced Very High Resolution Radiometer (AVHRR) and the High Resolution Infrared Sounder (HIRS). Along with these instruments, MHS is already in operation on the NOAA-18 satellite, which was launched in May 2005, and it also forms a part of the payload on NOAA-N' launched in 2008. MHS represents a significant enhancement in performance over the AMSU-B currently flying on the earlier NOAA-15,-16 and -17 satellites.

In conjunction with these U.S. instruments, the MHS instrument will provide improved data for weather prediction models with a resulting improvement in weather forecasting. MHS is intended primarily for the measurement of atmospheric humidity. It will measure cloud liquid water content. Furthermore, it will provide qualitative estimates of precipitation rate.

MHS helps to ensure the continuous and improved availability of operational meteorological observations from polar orbit whilst providing Europe with an enhanced capability for the routine observation of the Earth from space, and in particular, to further increase Europe's capability for long-term climate monitoring.

MHS instrument is a five-channel, self-calibrating microwave rotating radiometer on the nadir-facing side of the MetOp-A satellite and is designed to scan perpendicular to the direction flight (across track) at a rate of 2.67 s per scan. The swath width of the scan is approximately ±50°. The scan is synchronized with the AMSU-A1 and A2 instruments, with MHS performing three scan cycles for every one performed by the AMSU instruments.

The MHS incorporates four receiver chains at 89 GHz, 157 GHz and 190 GHz, with the 183-GHz data sampled in two discrete bands to provide the five channels. The fifth channel is achieved by splitting the 183.311 GHz signal into two channels, each with a different bandwidth.

Table A.13. Channel characteristics of the MHS.

Channel	Center Freq. (GHz)
1	89.0
2	157.0
3	183.311±1.0
4	183.311 ± 3.0
5	190.31

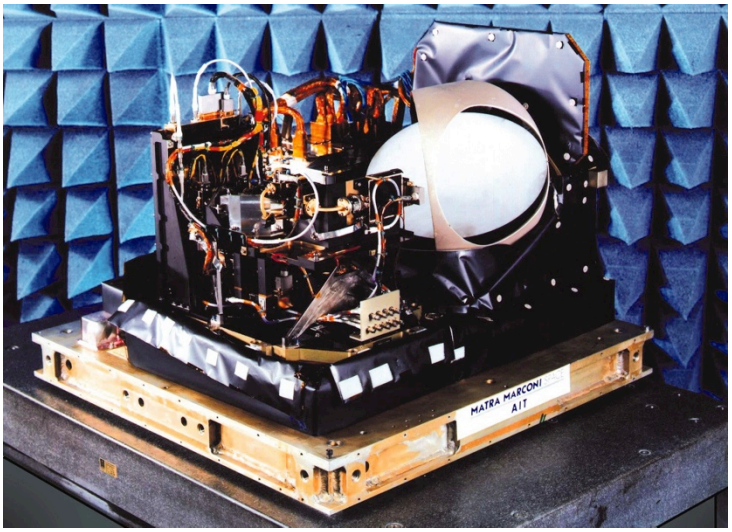

Fig. A.16. MHS instrument.

APPENDIX B : PREPROCESSOR AND GPROF2014 OUTPUT FORMATS

B.1 Preprocessor Output

B.1.1 Preprocessor Orbit Header

satellite	Character*12
sensor	Character*12
preprocessor version	Character*12
original radiometer file	Character*128
profile database file	Character*128
granule number	integer*4
number of scans	integer*4
number of pixels in scan	integer*4
number of channels with data	integer*4
channel frequencies	real(15)*4
channel errors	real(15)*4
comment	Character*44

note : channel_freq describes the exact frequencies of the channels, but they must be in the following order: 10v, 10h, 19v, 19h, 23v, 23h, 37v, 37h, 89v, 89h, 166v, 166h, 183_7v, 183_3v, 183_1v

B.1.2 Preprocessor Scan Header

ScanDate (6)	integer(6)*2	: year,month,day,hour,min,sec
Spacecraft latitude	real*4	
Spacecraft longitude	real*4	
Spacecraft altitude	real*4	

B.1.3 Preprocessor Data Record

Latitude		real*4
Longitude		real*4
Brightness temperatures		real(15)*4
Earth Incident angles		real(15)*4
Skin temp index		integer*2
2 Meter temperature index		integer*2
Sunglint angle	I	integer*1
Surface type code		integer*1
TCWV index		integer*1
Snow Cover Index		integer*1
Orographic Lifting Index		integer*1
Fill		integer(3)*1

B.2 GPM Precipitation Algorithm Output

Whether in the native, HDF formats, the output parameters will be equivalent. This following format description is for the GPM native output binary format file.

B.2.1 Orbit Header (at beginning of each file) (described in section 4.4.5)

Satellite	Character*12	
Sensor	Character*12	
Pre-processor Version	Character*12	
Algorithm Version	Character*12	
Profile Database Filename	Character*128	
Original Radiometer Filename	Character*128	
File Creation Date/Time(6)	integer*2	
Granule Start Date/Time(6)	integer*2	
Granule End Date/Time(6)	integer*2	
Granule Number	integer*4	
Number of Scans in Granule	integer*2	
Number of Pixels/Scan	integer*2	
Profile Structure Flag	integer*1	(0=no, 1 = yes)
Spares	51 bytes	

B.2.2 Vertical Profile Structure of the Hydrometeors (described in section 4.4.6)

Profile database partitioned by species and 2 meter air temperature. Nominally, there are 2100 possible unique profiles for each species, each with a general scale factor.

Number of Profile Species - Nspecies	integer*1	(4-6, defined in Species Description)
Number of Profile Temps - Ntemps	integer*1	(21, defined in Temp Description)
Number of Profiles Layers - Nlyrs	integer*1	(28, defined in HgtTopLayer)
Number of Clustered Profiles – Nprfs	integer*1	(100)
Species Description(Nspecies)	character*12	
Height, Top of Layers(Nlyrs)	integer*2	
Temperature Descriptions(Ntemps)	real*4	
Cluster Profiles(Nspecies,Ntemps,Nlyrs,Nprf)	real*4	

B.2.3 Scan Header (at beginning of each scan, described in section 4.4.7)

Spacecraft latitude	real*4
Spacecraft longitude	real*4
Spacecraft altitude (km)	real*4
Scan Date/Time (yr,mon,day,hour,min,sec,millisec)	integer*2
Spares	integer*2

B.2.4 Pixel Data (for each pixel in scan, described in section 4.4.8)

Pixel Status	integer*1	(one byte)
Retrieval Type	integer*1	
Quality Flag	integer*1	
Snow Cover Index	integer*1	Variables re-ordered for byte boundaries
Surface Type Index	integer*1	
Total Col Water Vapor Index	integer*1	Eliminated Emissivity Class
Orographic Lift Index	integer*1	variable
Database Expansion Index	integer*1	
Surface Skin Temperature Index	integer*2	
Sunglint Angle	integer*1	
Spare	integer*1	Added this spare byte
Latitude	real*4	
Longitude	real*4	
Surface Precipitation	real*4	
Liquid Precipitation Fraction	real*4	
Convective Precipitation Fraction	real*4	
Probability of Precipitation	real*4	
Most Likely Precipitation	real*4	
Precip 1st Tertial	real*4	
Precip 2nd Tertial	real*4	
Number of Significant Profiles	integer*2	
Spares	integer*2	
Rain Water Path	real*4	
Cloud Water Path	real*4	
Mixed Water Path	real*4	
Ice Water Path	real*4	
Temp2mIndex	integer*2	
Profile Number(5)	integer*2	this variable actually has 5 elements
Profile Scale(5)	real*4	changed to 5 species

B.2.5 Orbit Header Variable Description – total of 400 bytes

Satellite

Generally this is a character string for the satellite which produced the data. For example: GPM, MeghaTropics, DMSP-F10, TRMM, WNDSat

Sensor

Satellite Sensor, currently:
GPI, MAD, AMSR-E, SSM/I, SSMIS, TMI, WINDSAT, and others

PreProcessor Version

GPM Pre-Processor version number.

Algorithm Version

GPM Processing Algorithm Version which produced the output file.

Profile Database Filename

File name of the profile database. May be expanded to include multiple databases.

Original Radiometer Filename

File Name of the original, satellite observation input data file.

File Creation Date/Time

Start date and time of file creation. Defined as the date/time structure which holds six integer*2 values - year, month, day, hour, minute, second.

Granule Start Date/Time, End Date/Time

Start and End dates and times of first and last scan in file. Defined as the date/time structure, which holds year, month, day, hour, minute, second.

Granule Number

Generally this is defined as the satellite orbit number since launch.

Number of Scans in Granule, Number of Pixels per Scan

Number of sensor scans in the file, Number of pixels per scan for this sensor

Profile Structure Flag

Flag defining whether GPM Profiling Algorithm was run with vertical profiles of the hydrometeors. No structure = 0, with vertical structure = 1.

Spares

51 spare bytes for additional parameters.

B.2.6 Vertical Profile Variable Descriptions

These are always included even when the hydrometeor profiles are not computed. In this case the values will be set to missing. Section 4.6 describes the recovery of the retrieved hydrometeors profile using these profile variables.

Number of Profile Species

The number of different species. The character description of each is in the Species Description Variable below.

Number of Profile Temps

The number of profile temperature indicies. The exact values of the indices are given in the Temperature Description Variable below.

Number of Profiles Layers

Defined for GPM profiling algorithm as 28.

Number of Clustered Profiles

Number of unique profiles for each species and 2 meter Temperature index (100, nominally)

Species Description

Nspecies number of character descriptions of Species, e.g. "Cloud Water Content"

Hgt Top Layer

Height of the top of each 28 layers of GPM PA in kilometers (km). These are defined every 0.5 km up to 10 km, then every kilometer after that up to 18 km. Values are: 0.5, 1., 1.5, 2., 2.5, 3., 3.5,4.,4.5,5.,5.5, 6.,6.5,7., 7.5, 8., 8.5, 9., 9.5,10., 11., 12., 13., 14.,15., 16., 17., 18.

Temperature Descriptions

Values of Ntemps number of 2m temperature indexes, e.g. -24.0, -21.0, -19.0….

Cluster Profile Array

The array which holds the standard GPM profile structures.

B.2.7 Scan Variable Descriptions

Spacecraft latitude, Spacecraft longitude, Spacecraft altitude (km)

Satellite sub-point earth coordinate position and altitude

Scan Date/Time

Time at the beginning of the scan including milliseconds

Spares

2 spare bytes for a later additional parameter

B.2.8 Pixel Data Variable Descriptions

Pixel Status – a full list of these can only be created once the algorithm is finalized.

If there is no retrieval at a given pixel, pixelStatus explains the reason.

0 : Valid pixel

1 : Pixel out of Latitude/Longitude defined area
2 : Tbs out of range

Retrieval Type

Specifies that for this pixel, the rain retrieval was made with the S0, S1, or S2 (0,1,2).

Quality Flag

Quality Flag indicates a generalized quality of the retrieved pixel. Values follow:
Ocean Algorithm:

High: Good retrieval (uses only entries from apriori database)
Medium: Retrieval used extended parts of the database, or sunglint angle $<10^{o}$
Low: Retrieval used excessive search radius to find matches in profile database (see Database Expansion Index)

1 : Highest quality – (use it!)
2 : Medium quality (use with caution)
3 : Low quality (recommended qualitative use only)

Snow Cover Index

0-5 index on based on the snow depth. 0 = no snow, 2-5 increasing snow depth, the intervals are TBD.

Surface Type Index

Surface type codes are: 1 : Ocean, 2 : Sea ice, 3-7 : Decreasing vegetation, 8-11 : decreasing snow cover, 12: standing water, 13 : land/ocean or water coast, 14 : sea-ice edge, 15 = Land/Ice edge

Total Column Water Vapor Index

The integer total precipitable water (mm) used to select the correct database profiles.

Orographic Lift Index

Index of potential orographic enhancement to precipitation based on vertical motion, atmospheric moisture profile, wind direction, and terrain slope. Index values are TBD.

Database Expansion Index

This value is the expansion factor of the profile search radius in the profile database beyond the search nominal range. If there is fewer than the minimum number of profiles in the selected database boundaries, then the search radius is expanded. Values range from 0 – 255.

Surface Skin Temperature Index

The integer skin temperature from the model, used to select the correct database profiles.

Sun Glint Angle

Conceptually, the angle between the sun and the instrument view direction as reflected off the Earth's surface. sunGlintAngle is the angular separation between the reflected satellite view vector and the sun vector. When sunGlintAngle is zero, the instrument

views the center of the specular (mirror-like) sun reflection. Values range from 0 to 180 degrees. If this angle is < 10 degrees, the pixel is affected by sunglint and the pixels Quality Flag is lowered.

Latitude, Longitude

Pixel latitude and longitude.

Surface Precipitation

The instantaneous precipitation rate at the surface. Check pixelStatus for a valid retrieval. Values are in mm/hr.

Liquid Precipitation Fraction, and Convective Precipitation Fraction

The fraction of Surface precipitation with is liquid and Convective. Values are 0-1.

Probability of Precipitation

A diagnostic variable, in percent, defining the fraction of raining vs. nonraining Database profiles that make up the final solution. Values range from 0 to 100%.

Most Likely Precipitation

The surface precipitation value (mm/hr) with the highest occurrence within the Bayesian retrieval.

Precipitation 1st Tertial and 2nd Tertial

The surface precipitation value (mm/hr) at the 1st and 2nd tertiary of the precipitation distribution.

Number of Significant Profiles

The number of profiles used in the Bayesian average above 2 sigma. Profiles below this threshold are still used in the average, but are not included in this 'significant' profiles parameter.

Rain Water Path, Cloud Water Path, Mixed Water Path, and Ice Water Path

Total integrated rain water, cloud liquid water, mixed phase water and ice water in the vertical atmospheric column.

Profile Indexes: Temp2mIndex, Number, Scale

Profile Scale (one for each hydrometeor species), Profile Number, and Profile 2 meter temperature index, used as a reference into the corresponding cluster profile array. These define the correct hydrometeors profile for each pixel as described in section 4.6.

B.3 Hydrometeor Profile Recovery

In order to recover hydrometer profile values of a single pixel, use the profileNumber, profileScale and 2mTempindex parameters, select your species and loop over the levels by plugging these indices into the 'clusterprofile' array. Where:

S = species(1-4) 1 = cloud water content
2 = rain water content
3 = mixed water content
4 = ice water content

T = 2 meter temp index
L = profile level (1-28). The top of each level is specified in HgtTopLayer
P = profileNumber

Pixel value = ProfileScale(S) * clusterprofile(S,T,L,P)